Available online at www.sciencedirect.com
SCIENCE DIRECT®
Coordination Chemistry Reviews 249 (2005) 705–726
COORDINATION CHEMISTRY REVIEWS
www.elsevier.com/locate/ccr

Review

Strict self-assembly of polymetallic helicates: the concepts behind the semantics

Claude Piguet*, Michal Borkovec, Josef Hamacek, Kornelia Zeckert

Department of Inorganic, Analytical and Applied Chemistry, University of Geneva, 30 quai E. Ansermet, CH-1211 Geneva 4, Switzerland

Received 11 June 2004; accepted 24 August 2004

Dedicated to Professor Jean-Marie Lehn for his outstanding contribution to the field.

Contents

1. Introduction 705
2. Helicates as archetypes of self-assembled metallosupramolecular edifices 706
3. Strict self-assembly of helicates: a complicated thermodynamic process 709
4. The intimate mechanism of helicate self-assembly: the kinetic approach 714
5. Toward predictive strategies in helicate self assembly: the site-binding model 715
6. From helicates to multimetallic supramolecular architectures 721
   6.1. Infinite one-dimensional metallo-organic polymers 721
   6.2. Two-dimensional sandwich complexes 723
7. Conclusions and perspectives 725
Acknowledgement 725
References 725

Abstract

The theoretical and rational modelling of self-assembly processes is far less developed than the flourishing structural characterization of the resulting sophisticated and aesthetically appealing polymetallic architectures. However, an eventual predictive design based on molecular programming requires a detailed understanding of the chemical and physical concepts controlling self-assembly. Although the kinetic and thermodynamic background of multicomponent complexation processes remain suspicious to synthetic chemists, the recent development of two simple and complementary models for rationalizing the formation of polymetallic helicates opens the possibility of reliable predictions for the properties of multimetallic one-dimensional oligomers. The origin, theoretical base, and application of this approach for the modelling of helicates is discussed, together with its limitations and extensions toward multi-dimensional complexes.

Keywords: Self-assembly; Helicate; Thermodynamic; Cooperativity

1. Introduction

During the two last decades, research in coordination chemistry was dominated by the growth of metallo-supramolecular chemistry, which allows the preparation, isolation, and characterization of sophisticated multicomponents polymetallic oligomers [1]. The complexity of the latter (supra)molecular architectures corresponds to a considerable extension of the classical approach, which mainly focused on the investigation of monometallic complexes. There is no doubt that these advances are closely related

* Corresponding author. Tel.: +41 22 379 60 34; fax: +41 22 379 68 30.
E-mail address: claude.piguet@chiam.unige.ch (C. Piguet).

0010-8545/$ – see front matter © 2004 Elsevier B.V. All rights reserved.
doi:10.1016/j.ccr.2004.08.023

to the improvements of the characterization techniques with the implementation of (i) two-dimensional detectors in X-ray diffraction measurements, (ii) gradient fields in high-resolution NMR, and (iii) smooth ionization techniques in mass spectrometry [2]. However, the level of the theoretical rationalization does not follow these analytical developments, and only primitive predictive tools are used such (i) the matching between the rough stereochemical preferences of the metal ions and the ligand binding possibilities in molecular complexes [3], (ii) the maximization of site occupancy [4], and (iii) the combination of geometrical shapes in crystals and macroscopic edifices [5]. The origin of the craze of coordination chemists for self-assembly processes may be assigned to the report by Lehn et al. on the preparation of the first trimetallic double-stranded helicate $[Cu_3(\mathbf{L1})_2]^{3+}$ (Fig. 1) [6]. The subsequent introduction of new semantic terms, such as self-assembly, self-organization, self-recognition, cooperativity, algorithms, subroutines, etc. greatly helps in the rapid recognition of this new field and its dissemination [7]. At the same time, it hinders the use of classical thermodynamic and kinetic framework to rationalize these phenomena, thus leading to some reports on debatable strategies, in which several components are combined to produce sophisticated edifices without involving thermodynamic intermediates or competitive pathways [1–3].

Nevertheless, fascinating novel topologies and (supra)molecular architectures become accessible (Fig. 2) [1], together with a panel of useful molecular functions working at the microscopic level [8]. In this review, we focus on thermodynamic and kinetic concepts, which describe self-assembly processes, in order to highlight the link between classical coordination chemistry and metallosupramolecular chemistry. The different approaches for rationalizing the self-assembly of one-dimensional polymetallic helical oligomers, i.e. the helicates [2,6] are presented together with two complementary simple predictive thermodynamic models.

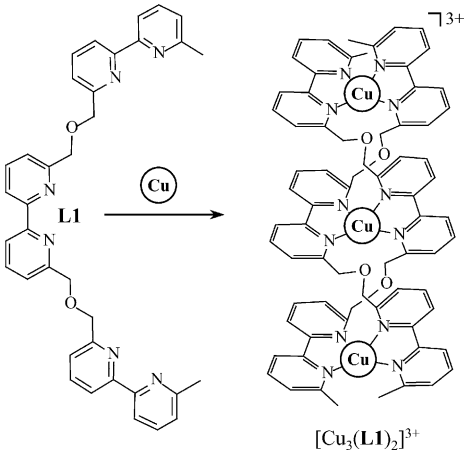

Fig. 1. Self-assembly of the trimetallic double-stranded helicate $[Cu_3(\mathbf{L1})_2]^{3+}$ [6].

2. Helicates as archetypes of self-assembled metallosupramolecular edifices

Since the first observation of a bimetallic triple-stranded complex [9], and its subsequent definition as 'helicate' (i.e. a discrete helical supramolecular complex constituted by one or more covalent organic strands wrapped about and coordinated to a series of ions defining the helical axis) [2,6], a huge number of polymetallic structures fulfilling these criteria has been reported [2,10]. In two seminal contributions, Lehn et al. introduced the terms 'self-assembly' [11] and 'self-recognition' [12] which are intimately linked with thermodynamics. Firstly, the relationship between the number of bidentate bipyridine units in **L2** (two segments), **L3** (three segments), **L4** (four segments) and **L5** (five segments), and the selective formation of bimetallic $[Cu_n(\mathbf{Ln})_2]^{n+}$ (n = 2), trimetallic (n = 3), tetrametallic (n = 4) and pentametallic (n = 5) double-stranded helicates (Fig. 3) can be rationalized with the consideration that the largest translational entropy results from the formation of a maximum number of short saturated oligomers [11,13]. This entropic aspect can be further strengthened by the judicious tuning of the relative stoichiometries and total concentrations of the components [14]. Secondly, the formation of the maximum number of dative bonds in the final helicates obviously contributes to minimize the free energy of complexation (enthalpic contribution, Fig. 4) [12]. The latter concept is often referred to as 'the principle of maximum occupancy' [4]. The combination of these enthalpic and entropic contributions qualitatively explains the recognition processes occurring when (i) a mixture of **L2**–**L5** reacts with Cu(I) to give exclusively the homopolymetallic helicates $[Cu_n(\mathbf{Ln})_2]^{n+}$ (n = 2–5, Fig. 3) [12], (ii) a mixture of **L1** and **L6** selectively sorts out Cu(I) and Ni(II) to give double-stranded $[Cu_3(\mathbf{L1})_2]^{3+}$ and triple-stranded $[Ni_3(\mathbf{L6})_3]^{6+}$ helicates (Fig. 4) [12], and (iii) a

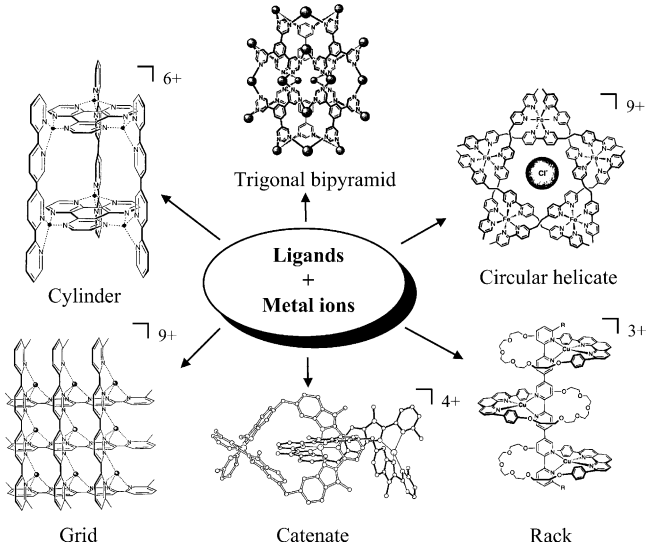

Fig. 2. Selected metallosupramolecular complexes obtained by self-assembly.

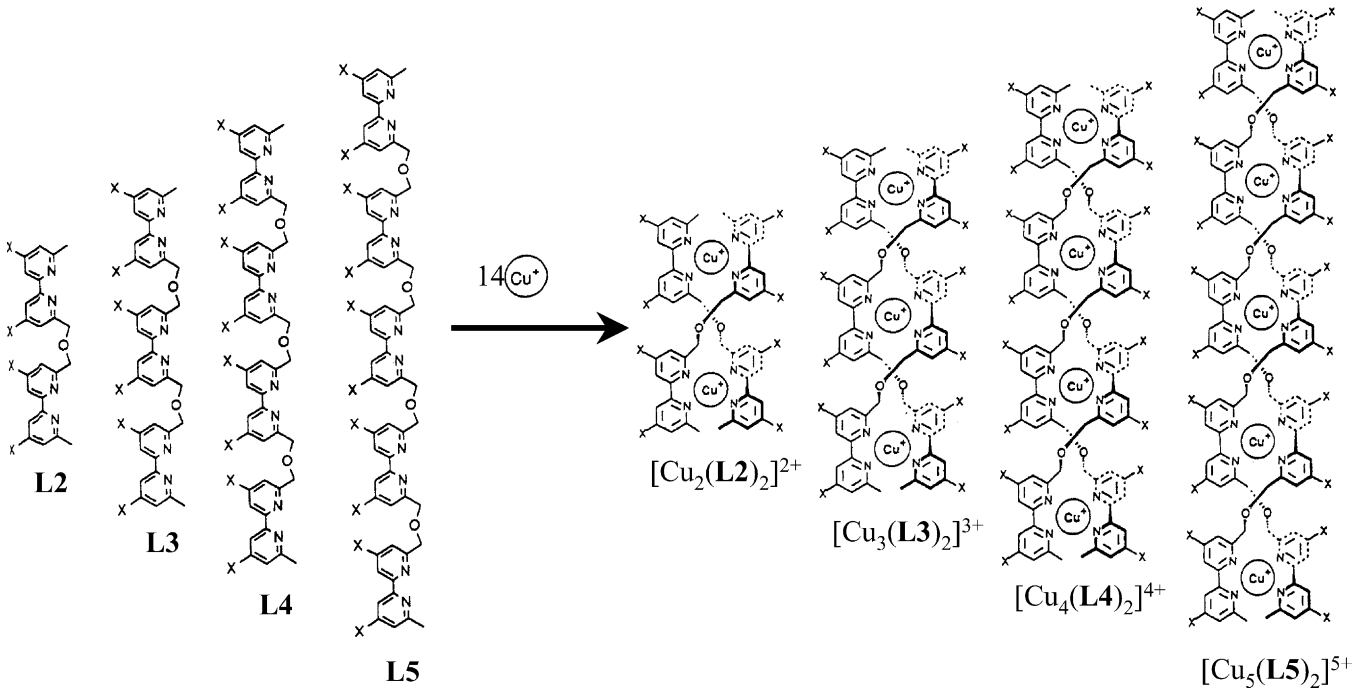

Fig. 3. Self-recognition of the homopolymetallic double-stranded helicates $[Cu_n(\mathbf{Ln})_2]^{n+}$ (n = 2–5, adapted from [12]).

mixture of **L7**–**L9** coordinates to Ga(III) to give the homoleptic bimetallic triple-stranded helicates $[Ga_2(\mathbf{Ln}\text{-}4H)_3]^{6-}$ (n = 7–9, Fig. 5) [14].

The discrimination exhibited in Fig. 4 points toward an underlying chemical 'algorithm' involving the ligand binding possibilities and the stereochemical preferences of the metal ions to give programmed helical complexes with predetermined structures and nuclearities [7]. On the other hand, the detection of considerable quantities of the heteroleptic double-stranded helicates $[Cu_3(\mathbf{L10})(\mathbf{L11})]^{3+}$ [15] and $[M_2(\mathbf{L12})(\mathbf{L13})]^{4+}$ (M = Ni, Cu, Zn) [16] during the sorting processes of **L10**/**L11** or **L12**/**L13** pairs, points to the thermodynamic limits of self-recognition events, which indeed require sufficient structural and electronic differences

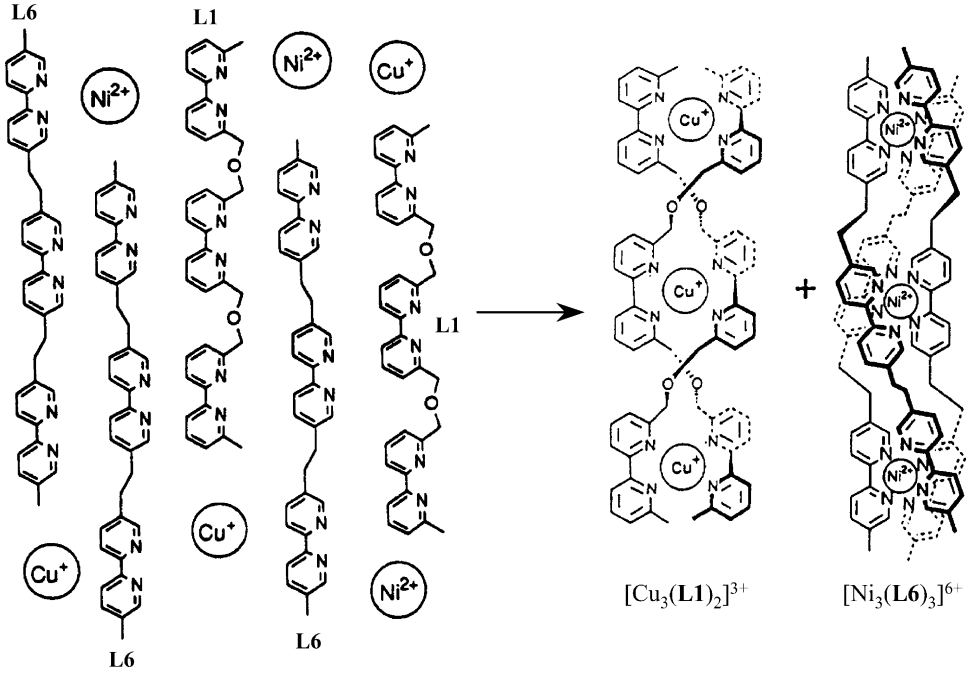

Fig. 4. Self-recognition of the double-stranded helicate $[Cu_3(\mathbf{L1})_2]^{3+}$ and the triple-stranded helicate $[Ni_3(\mathbf{L6})_3]^{6+}$ (adapted from [12]).

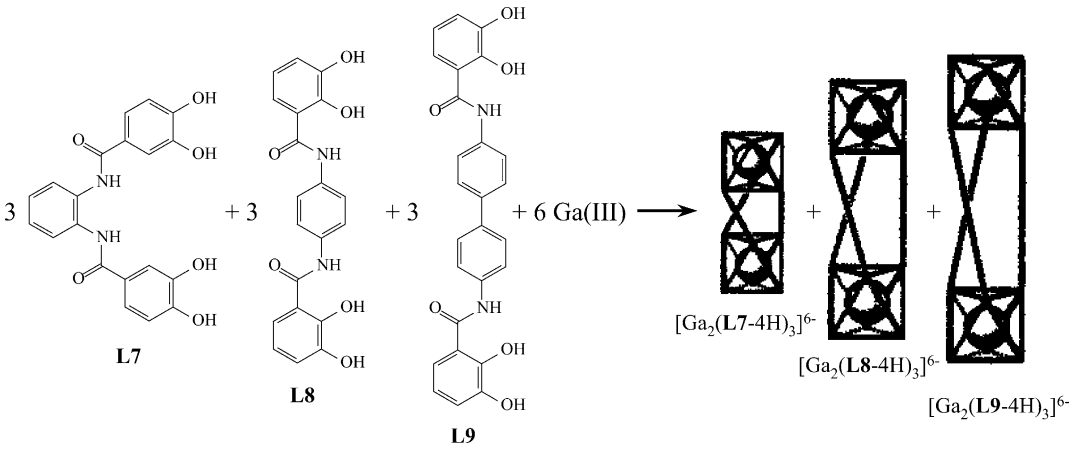

Fig. 5. Self-recognition of the homoleptic triple-stranded helicates $[Ga_2(\mathbf{L}n\text{-}4H)_3]^{6-}$ (n = 7–9, adapted from [14]).

between the binding possibilities of the ligand strands to provide efficient discrimination.

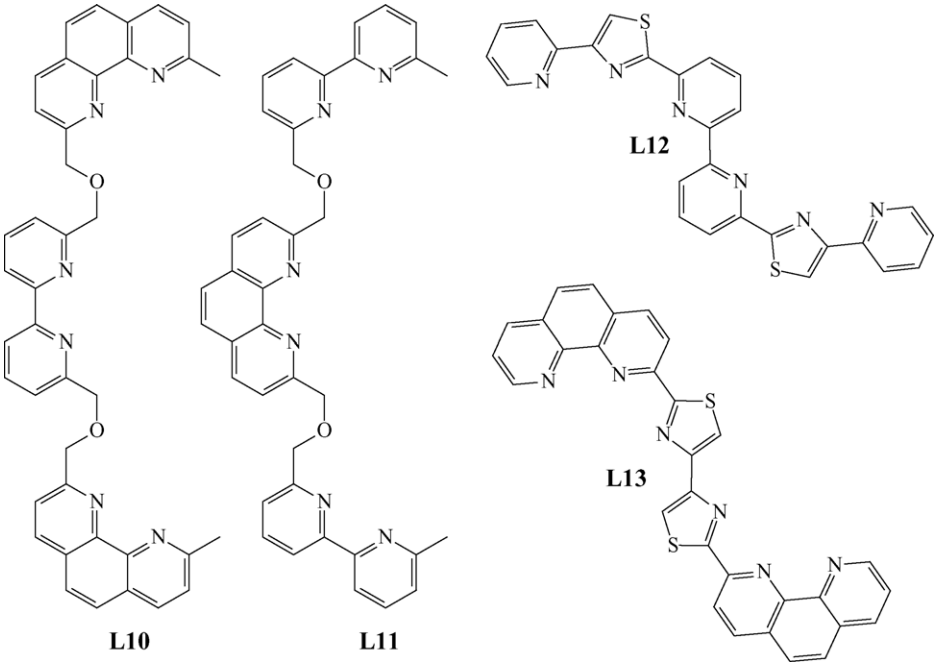

Assuming that 'algorithms' may be implemented in helicate self-assembly, the reading of the information encoded within the successive segments along the ligand strands may be selectively performed by a judicious choice of metal ions evidencing specific stereoelectronic preferences. As a result of their large covalent contributions and variable ligand-field stabilization energies, the first heterometallic helicates used mixtures of tetrahedral (Cu(I) or Ag(I)) and octahedral (Fe(II) or Co(II)) d-block ions. Reaction of mixtures of the latter ions with heterotopic segmental ligands possessing adjacent bidentate diimines (coded for tetrahedral metal ions) and tridentate terimines (coded for octahedral metal ions) produces pure heterometallic double-stranded helicates [17]. According to an analogous strategy, the ligand **L14** combines a α,α′-diimine unit (coded for a soft d-block ion) with a tridentate segment (coded for a hard 4f-block ion). Reaction with a mixture of labile pseudo-octahedral M(II) (M = Cr, Fe, Co, Ni) and spherical Ln(III) (Ln = La–Lu) ions shows the quantitative formation of the C_3-symmetrical heterobimetallic d–f triple-stranded helicates HHH-$[LnM(\mathbf{L14})_3]^{5+}$, in which each strand adopts a relative parallel orientation (HHH stands for 'head-to-head-to-head', which characterizes the parallel orientation of the three strands, Fig. 6) [18]. Although the absence of the HHT isomer (head-to-head-to-tail) may appear as a virtue of self-assembly, the thorough exploration of the energy hypersurface of the assembly process demonstrates that any deviation from exact stoichiometric conditions and high concentration results in the formation of various alternative homometallic complexes (Fig. 6).

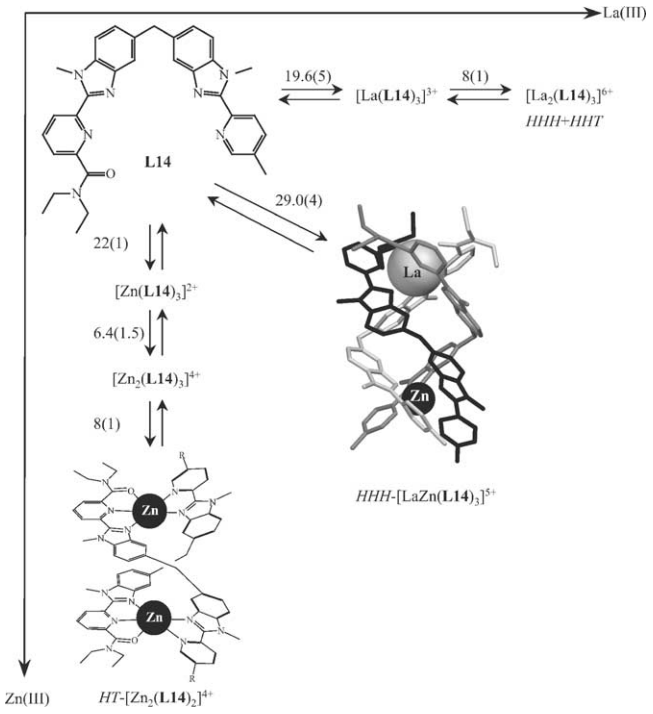

Fig. 6. Strict self-assembly of the heterobimetallic d–f triple-stranded helicate HHH-[LaZn(**L14**)$_3$]$^{5+}$ in acetonitrile (numerical values correspond to log(β) for the thermodynamic equilibrium) [18a].

The situation becomes even more challenging for the preparation of heterometallic f–f′ helicates because of the extreme similarity of the coordination behaviour of f-block ions along the lanthanide series. To the best of our knowledge, the bis-tridentate heterotopic **L15** is the unique example, in which partial selectivity (i.e. a deviation from a binomial distribution) favors the formation of heterobimetallic f–f′ helicates: [Ln^{1}Ln^2(**L15**)$_3$]$^{6+}$ (Fig. 7) [19]. Although competition between C_3-symmetrical HHH and C_1-symmetrical HHT isomers for both homo- and heterobimetallic helicates prevents a clear picture of the origin of the recognition process, the detection of 90% of HHH-[LaLu(**L15**)$_3$]$^{6+}$ in solution is an undeniable success of strict self-assembly (i.e. 'strict' stands for thermodynamically driven) [11b].

The level of the theoretical description of the assembly process has thus become one of the limiting factors for further developments in helicate self-assembly, and two opposite research strategies have been implemented. Firstly, highly sophisticated and aesthetically appealing entwined polymetallic architectures have been isolated from intricate mixtures assuming that the rough rationalization brought by the 'algorithm' approach is sufficient. Beyond the original double- and triple-stranded helicates, talented chemists were able to prepare attracting quadruple-stranded [20], single-stranded circular [21], double-stranded circular [22] and alternated circular [16] helicates, together with even more complicated three-dimensional assemblies containing variable ratios of grid-like and helical-like portions (Fig. 8) [23].

The second strategy focus on the re-examination of the underlying thermodynamic and kinetic background in order to build simple tools for predicting supramolecular structures. In this context, the considerable amount of data collected for the strict self-assembly of helicates can be used for the validation of theoretical models. Although the structural and preparative approaches leading to self-assembled helicates have been regularly and comprehensively reviewed during the last decade [1,2,10], little attention has been paid to the global presentation and discussion of thermodynamic and kinetic concepts, which are the topic of this review.

3. Strict self-assembly of helicates: a complicated thermodynamic process

The first quantitative thermodynamic study describing the self-assembly of a helicate can be attributed to Williams and co-workers [24] who reported the formation of the triple-stranded bimetallic helicate [Co$_2$(**L16**)$_3$]$^{4+}$ (log(β_{23}) = 21.4(6)), which apparently does not involve any thermodynamic intermediate in significant amounts. The reaction of the same ligand **L16** with pseudo-tetrahedral Cu(I) eventually provides the double-stranded helicate [Cu$_2$(**L16**)$_2$]$^{2+}$ (log(β_{22}) = 13.0(3)), but the formation of a 1:2 intermediate [Cu(**L16**)$_2$]$^+$ (log(β_{12}) = 8.5(3)) is established during the titration process. The lack of

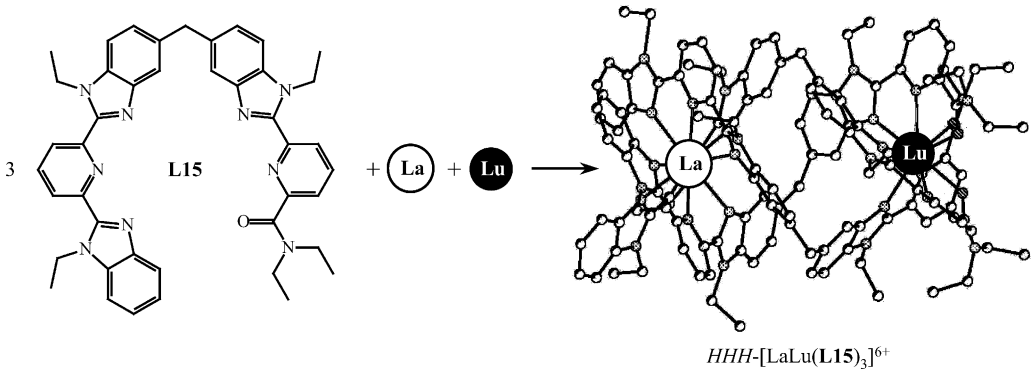

Fig. 7. Partial description of the strict self-assembly of the heterobimetallic f–f′ triple-stranded helicate HHH-[LaLu(**L15**)$_3$]$^{6+}$ in acetonitrile [19].

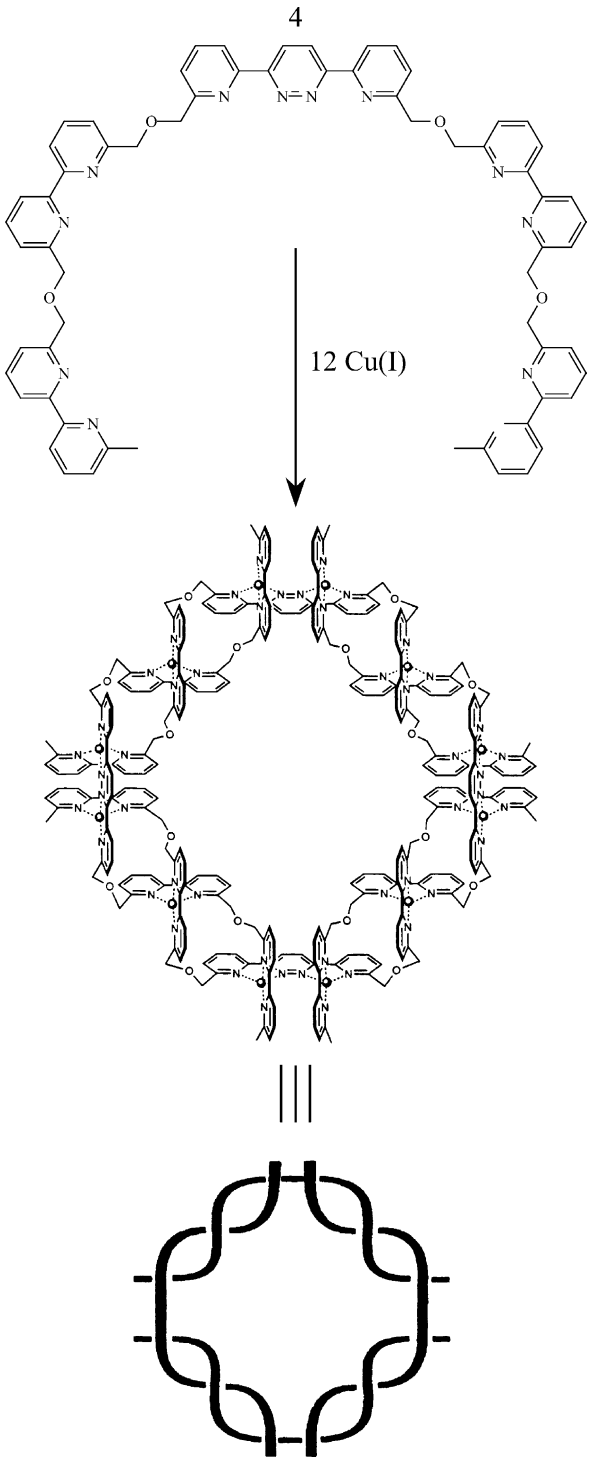

Fig. 8. Self-assembly of a sophisticated polymetallic entwined oligomer. Adapted from [23].

evidence for potential intermediates, such as $[Co(\mathbf{L16})_3]^{2+}$ or $[Co(\mathbf{L16})_2]^{2+}$ in the former process led these authors to suggest the occurrence of a strongly positive cooperative process, but no quantitative argument supports this hypothesis [24].

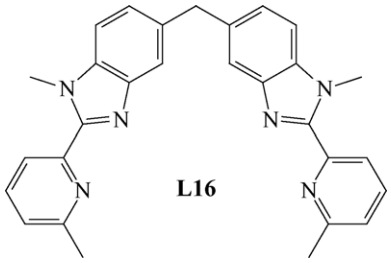

In a related study, Lehn and co-workers reported on the thorough thermodynamic charaterization of the self-assembly of the trimetallic double-stranded helicate $[Cu_3(\mathbf{L3})_2]^{3+}$ (equilibria (1)–(4)) [25].

$$Cu^+ + \mathbf{L3} \rightleftharpoons [Cu(\mathbf{L3})]^+, \quad \log(\beta_{11}) = 4.6(1) \tag{1}$$

$$Cu^+ + 2\mathbf{L3} \rightleftharpoons [Cu(\mathbf{L3})_2]^+, \quad \log(\beta_{12}) = 8.2(2) \tag{2}$$

$$2Cu^+ + 2\mathbf{L3} \rightleftharpoons [Cu_2(\mathbf{L3})_2]^{2+}, \quad \log(\beta_{22}) = 13.5(2) \tag{3}$$

$$3Cu^+ + 2\mathbf{L3} \rightleftharpoons [Cu_3(\mathbf{L3})_2]^{3+}, \quad \log(\beta_{23}) = 18.6(2) \tag{4}$$

Assuming that the thermodynamic protein/ligand model is adequate for the description of this assembly process [26], simple graphical tests for cooperativity (*Scatchard* plots [27] and *Hill* plots [28]) suggest strong positive cooperativity, despite the expected electrostatic repulsion occurring between charged cations (Fig. 9) [25].

However, as pointed out by Ercolani [29], the formation constants of equilibria (1)–(4) possess different dimensions arising from the combination of intra- and intermolecular complexation processes involving different components, and they cannot be easily interpreted. Consequently, the protein/ligand model, which explicitely requires only virtually identical intermolecular processes (i.e. the successive binding of one component to a preassembled receptor, Fig. 10), cannot be used without further adaptations in metallosupramolecular chemistry. Moreover, the interpretation of *Scatchard* or *Hill* plots for multicomponent assemblies remains elusive without the adequate theoretical support. Prior to develop thermodynamic models for rationalizing the formation of self-assembled polymetallic helicates, it is worth to focus on the term 'cooperativity' and its specific use and meaning in coordination chemistry and in metallosupramolecular chemistry.

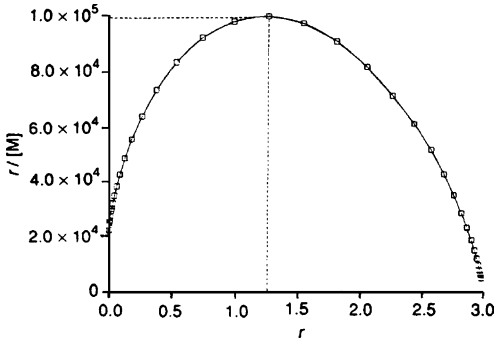

Fig. 9. Scatchard plot for the formation of the double-stranded helicate $[Cu_3(\mathbf{L3})_2]^{3+}$ [25a]. Reproduced with permission from [25a], copyright Royal Society of Chemistry, 1992.

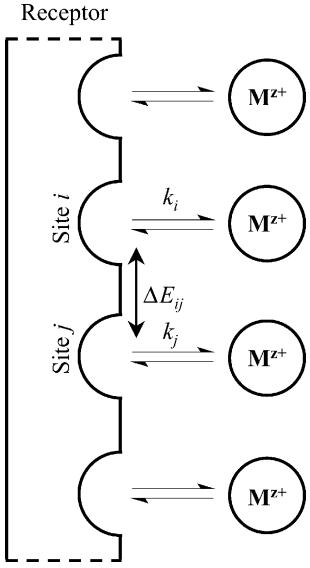

Fig. 10. Thermodynamic model for the fixation of metal ions to an one-dimensional multi-site receptor.

For the coordination of metal ions (or protons, or ligands) to a preassembled receptor possessing n sites, cooperativity is unambigously ascribed to the interaction free energy ΔE_{ij} (corrected for statistics) between metal ions i and j (Fig. 10) [26,30]. When $\Delta E_{ij} = 0$, the fixation of one metal ion in site i has no influence on the coordination of an other metal to site j, and the binding is non-cooperative. When $\Delta E_{ij} \neq 0$, the fixation of a metal ion in site i favors ($\Delta E_{ij} < 0$) or hinders ($\Delta E_{ij} > 0$) the fixation of the second metal ion in site j, thus leading to *positive* or *negative cooperativity*, respectively. In the two latter cases, significant deviations from a pure statistical approach occur. Obviously, the permutation of the 'metal' and 'ligand' labels does not alter the thermodynamic model. Therefore, the successive fixation of n ligands to a metal (considered as the preassembled receptor) obeys the same rules assuming that ΔE_{ij} stands for the interligand interaction.

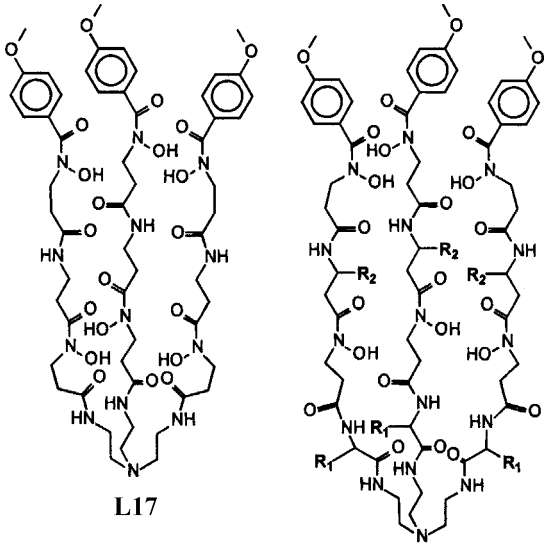

L17 **L18**

The simple model depicted in Fig. 10 thus applies for the successive fixation of Fe(III) to the C_3-symmetrical podands **L17** and **L18** (equilibria (5) and (6)) [31].

$$\mathbf{L}\boldsymbol{i} + \text{Fe(III)} \rightleftharpoons [\text{Fe}(\mathbf{L}\boldsymbol{i})], \quad i = 17, 18, \quad K_1 \tag{5}$$

$$[\text{Fe}(\mathbf{L}\boldsymbol{i})] + \text{Fe(III)} \rightleftharpoons [\text{Fe}_2(\mathbf{L}\boldsymbol{i})], \quad i = 17, 18, \quad K_2 \tag{6}$$

If we approximate that the two pseudo-octahedral hexadentate binding sites in **L17** are equivalent, the statistical ratio in absence of cooperativity ($\Delta E = 0$) amounts to $K_2/K_1 = 1/4 = 0.25$ [26]. The significant experimental deviation $(K_2/K_1)_{\text{exp}} = 3.2$ observed for **L17** implies that $\Delta E < 0$, and that positive cooperativity occurs as a result of the efficient charge compensation provided by the polyhydroxamate ligand combined with the formation of a peripheral belt of hydrogen bonds accompanying the complexation processes [31]. For the larger ligand **L18**, the hydrogen bonding is less efficient in preorganizing the strands for the second complexation event, and a non-cooperative process occurs ($(K_2/K_1)_{\text{exp}} \approx 0.25$ and $\Delta E = 0$) [31].

In metallosupramolecular chemistry, the use of the term 'cooperativity' is different because the self-assembly processes mix inter- and intramolecular processes involving various components. Unfortunately, this term is systematically invoked when the *repetitive binding of metal ions* (or protons or ligands) *in equivalent sites occurs with a fixed interaction parameter*. In other words, it is sufficient that ΔE_{ij} does not vary during the successive complexation processes leading to the final multimetallic supramolecular architectures. Consequently, $\Delta E_{ij} \neq 0$ is fully compatible with the supramolecular concept of 'non-cooperativity', according that it remains constant during the complete growing process of the final structure [25,29]. In order to clarify the situation and to better differentiate these two phenomena, we will restrict the use of the concept of *cooperativity* to the explicit interpretation of the value ΔE_{ij}, as it is used in thermodynamics [26], and we introduce the new terminology of *statistical repetitive binding* for the successive filling of coordination sites occurring with a fixed interaction parameter. This second concept (i.e. statistical repetitive binding) is of interest for rationalizing multi-component self-assembly processes in which intra- and intermolecular processes concomitantly operate. It has been developed by Ercolani for the general case of a self-assembly process in which l metals M coordinate to m receptors L, having l equivalent binding sites (equilibrium (7)) [29].

$$m\text{L} + l\text{M} \rightleftharpoons [\text{M}_l\text{L}_m], \quad \beta_{lm} \tag{7}$$

$$\beta_{ml} = \delta\sigma_{\text{sa}} K_{\text{inter}}^{N-1} K_{\text{intra}}^{B-N+1} \tag{8}$$

The associated formation constant β_{lm} is given by Eq. (8) in which (i) δ is the contribution of the entropy of mixing for the formation of enantiomers from achiral receptors (chirality factor) [32], (ii) $\sigma_{\text{sa}} = \sigma_{\text{L}}^{m}\sigma_{\text{M}}^{l}/\sigma_{\text{Complex}}$ is the symmetry factor of the self-assembly equilibrium (7) [32], (iii) K_{inter} is the microscopic equilibrium constant associated with the reference intermolecular reaction occurring between

monofunctional reactants, (iv) K_{intra} is the microscopic (statistically corrected) constant associated with the subsequent intramolecular reaction processes, (v) $N = m + l$ is the total number of components in the complex, and (vi) $B = ml$ is the number of connections joining the components in the latter complex [29].

Since the two six-coordinate binding sites in **L17** and **L18**, are not strictly equivalent, Eq. (8) does not hold, but we can reasonably assume (i) ideal chiral D_3 symmetry for **L*i*** ($\sigma_L = 6$) and [Fe$_2$(**L*i***)] ($\sigma_{Complex} = 6$), and (ii) C_3-symmetry for [Fe(**L*i***)] ($\sigma_{Complex} = 3$). In these conditions, the application of Eq. (8) for analyzing the formation of [Fe(**L*i***)] (equilibrium (5), $\delta = 1$) and [Fe$_2$(**L*i***)] (equilibrium (9), $\delta = 1$) leads to Eqs. (10) and (11), respectively, in which only successive intermolecular processes are involved in complete agreement with the classical protein/ligand model (Fig. 10) [26]. The subsequent calculation of $K_2 = \beta_{21}/\beta_{11}$ leads to the expected statistical criterion $K_2/K_1 = \beta_{21}/(\beta_{11})^2 = 1/4 = 0.25$ when no interaction occurs between the sites.

$$\mathbf{L}i + 2\mathrm{Fe(III)} \rightleftharpoons [\mathrm{Fe}_2(\mathbf{L}i)], \quad i = 17, 18, \quad \beta_{21} \tag{9}$$

$$\beta_{11} = K_1 = 2K_{inter} \tag{10}$$

$$\beta_{21} = K_{inter}^2 \tag{11}$$

In other words, *Ercolani*'s model obviously accounts for the simple case of successive intermolecular complexation processes (i.e. the protein/ligand model), but it is more general since sophisticated self-assembly processes involving intricate inter- and intramolecular processes can be analyzed with the same approach.

According to *Ercolani*'s model, the application of Eq. (8) for analysing the formation constant β_{m2} of *Lehn*'s double-stranded helicates [Cu$_m$(**L3**)$_2$]$^{m+}$ (equilibrium (12)) is given by Eq. (13) ($N = m + 2$ components and $B = 2m$ connections between them) [29].

$$m\mathrm{Cu}^+ + 2\mathbf{L3} \rightleftharpoons [\mathrm{Cu}_m(\mathbf{L3})_2]^{m+}, \quad \beta_{m2} \tag{12}$$

$$\beta_{m2} = \delta\sigma_{sa}\, K_{inter}^{m+1}\, K_{intra}^{m-1} \tag{13}$$

$\sigma_{sa} = \sigma_{L3}^2\, \sigma_{Cu}^m/\sigma_{Complex}$ is the symmetry factor of the self-assembly equilibrium (12) ($\sigma_{Metal} = 1$, $\sigma_{Ligand} = 2$ and $\sigma_{Complex}$ depends on its symmetry point group: $\sigma_{Complex} = 1$ for C_1-symmetry, $\sigma_{Complex} = 2$ for C_2-symmetry and $\sigma_{Complex} = 4$ for D_2-symmetry) [32], K_{inter} is the microscopic intermolecular equilibrium constant associated with the formation of [Cu(**L3**)]$^+$ taken as a reference, K_{intra} is the microscopic (statistically corrected) intramolecular constant associated with the subsequent complexation of Cu(I) to [Cu(**L3**)$_2$]$^+$ to give [Cu$_m$(**L3**)$_2$]$^{m+}$. The application of Eq. (13) for the formation of [Cu(**L3**)$_2$]$^+$ (equilibrium (2), β_{12}) requires the consideration of three different arrangements (i.e. three microscopic constants) and leads to Eq. (14) from which K_{inter} can be calculated. Eq. (15) holds for the two microscopic constants characterizing [Cu$_2$(**L3**)$_2$]$^{2+}$ (equilibrium (3), β_{22}) from which K_{intra} can be eventually computed [29].

$$\beta_{12} = 9(K_{inter})^2 \tag{14}$$

$$\beta_{22} = 8(K_{inter})^3 K_{intra} \tag{15}$$

Assuming that (i) the three bipyridine segments in **L3** have identical absolute affinities for Cu(I), and (ii) statistical repetitive binding holds (i.e. ΔE_{ij} is constant), the statistical formation constant β_{32}^{stat} for the trimetallic helicate [Cu$_3$(**L3**)$_2$]$^{3+}$, (equilibrium (4)) can be estimated by applying Eq. (13). Eq. (16) results and comparison of $\log(\beta_{32}^{stat}) = 18.25$ [29] with the experimental constant $\log(\beta_{32}) = 18.6(2)$ (equilibrium (4)) [25] shows only a negligible deviation within experimental error.

$$\beta_{32}^{stat} = 2(K_{inter})^4(K_{intra})^2 \tag{16}$$

Ercolani deduces that statistical repetitive binding occurs (termed 'non-cooperativity' in the original paper [29]) in contrast with the original suggestion of positive deviation from statistics favouring the formation of the multimetallic edifice [25]. However, this approach does not allow the quantitative estimation of the interaction parameter ΔE_{ij}, but it debunks some 'magical' aspects often associated with self-assembly processes in metallosupramolecular chemistry.

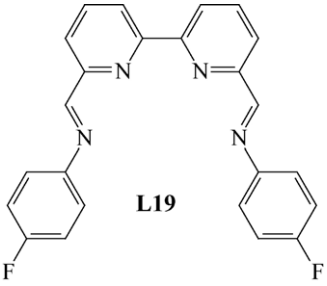

L19

The reaction of ligand **L19** with Cu(I) to give the double-stranded helicate [Cu$_2$(**L19**)$_2$]$^{2+}$ represents the second helicate system in which thermodynamic data have been interpreted in term of 'positive cooperativity' (equilibria (17)–(19)) [33].

$$\mathrm{Cu}^+ + \mathbf{L19} \rightleftharpoons [\mathrm{Cu}(\mathbf{L19})]^+, \quad \log(\beta_{11}) = 5.30 \tag{17}$$

$$\mathrm{Cu}^+ + 2\mathbf{L19} \rightleftharpoons [\mathrm{Cu}(\mathbf{L19})_2]^+, \quad \log(\beta_{12}) = 11.60 \tag{18}$$

$$2\mathrm{Cu}^+ + 2\mathbf{L19} \rightleftharpoons [\mathrm{Cu}_2(\mathbf{L19})_2]^{2+}, \quad \log(\beta_{22}) = 26.47 \tag{19}$$

Although the authors notice the ambivalent binding nature of **L19**, which may act as a terminal or as a central bidentate α,α′-diimine binding unit, they arbitrarily use the criterion $K_{12}/\beta_{11} > 1$ (equilibria (17) and (20)) for asserting that the successive complexation of two ligands to Cu(I) occurs with positive cooperativity [33].

$$[\mathrm{Cu}(\mathbf{L19})]^+ + \mathbf{L19} \rightleftharpoons [\mathrm{Cu}(\mathbf{L19})_2]^+,$$

$$\log(K_{12}) = \log(\beta_{12}) - \log(\beta_{11}) = 6.30 \tag{20}$$

Since equilibria (17) and (20) correspond to virtually identical chemical events involving only intermolecular processes (K_{inter}), they can be indeed directly compared, but a reliable

criterion for cooperativity must consider all the possible arrangements adopted by $[Cu(\mathbf{L19})]^+$ and $[Cu(\mathbf{L19})_2]^+$. Firstly, the 1:1 complex $[Cu(\mathbf{L19})]^+$ may exist either as a non-chiral C_s-symmetrical isomer in which Cu(I) is bound to the terminal imino-pyridine bidentate segment (δ = 1 and $\sigma_{sa} = \sigma_{Ligand}\sigma_{Metal}/\sigma_{Complex} = 2$ for equilibrium (17)) [32], or as a non-chiral C_{2v}-symmetrical isomer in which Cu(I) is bound to the central bipyridine segment (δ = 1 and σ_{sa} = 1 for equilibrium (17)) [29,32]. The use of Eq. (8) [29] provides the modelling of the macroscopic constant β_{11} as the sum of the two microscopic constants associated with each isomer (Eq. (21)).

$$\beta_{11} = 2K_{inter} + K_{inter} = 3K_{inter} \quad (21)$$

The same approach applied to equilibrium (18) requires the consideration of three different isomers for $[Cu(\mathbf{L19})_2]^+$. (i) A chiral C_2-symmetrical complex in which Cu(I) is coordinated by two terminal imino-pyridine bidentate segments (δ = 2 and σ_{sa} = 2 for equilibrium (18)) [32]. (ii) A chiral C_1-symmetrical complex in which Cu(I) is coordinated by one terminal imino-pyridine and by one central bipyridine segments (δ = 2 and σ_{sa} = 4 for equilibrium (18)) [32]. (iii) A non-chiral D_{2d}-symmetrical complex in which Cu(I) is coordinated by the two central bipyridine segments (δ = 1 and σ_{sa} = 1 for equilibrium (18)) [32]. The systematic use of Eq. (8) [29] for each isomer provides three microscopic constants which can be combined to give the macroscopic constants β_{12} (Eq. (22)).

$$\beta_{12} = 4(K_{inter})^2 + 8(K_{inter})^2 + (K_{inter})^2 = 13(K_{inter})^2 \quad (22)$$

The value K_{12} is then calculated by using equilibrium (20) in which $K_{12} = \beta_{12}/\beta_{11}$ (Eq. (23)).

$$K_{12} = \tfrac{13}{3}K_{inter} \quad (23)$$

We can easily deduce from Eqs. (21) and (23) that deviations from the statistical ratio K_{12}/β_{11} = 13/9 = 1.44 is the correct criterion for the successive non-cooperative binding of two ligand strands **L19** to Cu(I). The experimental ratio $K_{12}^{exp}/\beta_{11}^{exp} = 10 \gg 1.44$ reveals significant deviation, and it is diagnostic for successive ligand binding driven by positive cooperativity (i.e. $\Delta E_{ij} < 0$ for interligand interactions in $[Cu(\mathbf{L19})_2]^+$). However, nothing can be deduced for a possible deviation from statistical repetitive binding leading to the final chiral D_2-symmetrical bimetallic double-stranded helicate $[Cu_2(\mathbf{L19})_2]^{2+}$ (δ = 2 and σ_{sa} = 1 for equilibrium (19)) because β_{22} depends on both intermolecular (K_{inter}) and intramolecular (K_{intra}) processes (Eq. (24)).

$$\beta_{22} = 2(K_{inter})^3 K_{intra} \quad (24)$$

From the experimental data obtained for β_{12} (equilibrium (18)) and β_{22} (equilibrium (19)), K_{inter} (Eq. (22)) and K_{intra} (Eq. (24)) can be easily estimated, but these constants are of limited interest since the predictions for the formation of the next higher trimetallic homologue cannot be compared with experimental data [33]. Nevertheless, a second arbitrary criterion $K_{22}/K_{12} > 1$ (equilibria (20) and (25)) has been used in reference [33] for tentatively assigning positive cooperativity for the global thermodynamic process. The combination of Eq. (22) (β_{12}) and Eq. (24) (β_{22}) allows the evaluation of K_{22} for equilibrium (25), and the final result is given in Eq. (26).

$$[Cu(\mathbf{L19})_2]^+ + Cu^+ \rightleftharpoons [Cu_2(\mathbf{L19})_2]^+,$$

$$\log(K_{22}) = \log(\beta_{22}) - \log(\beta_{12}) = 14.87 \quad (25)$$

$$K_{22} = \tfrac{2}{13}K_{inter}\,K_{intra} \quad (26)$$

The ratio K_{22}/K_{12} = (6/169)K_{intra} can be then easily deduced when considering Eqs. (23) and (26). In other words, the latter ratio depends on K_{intra} and cannot be considered as a reliable criterion for testing the occurrence of a statistical repetitive binding process in $[Cu_2(\mathbf{L19})_2]^{2+}$. We conclude that the system Cu(I)/**L19** indeed displays positive cooperativity for the successive fixation of the two strands to one Cu(I) (i.e. $\Delta E < 0$), but no conclusion can be drawn concerning the statistical successive binding of the metal ions. This limitation emanates from the explicit separation of inter- and intramolecular processes in metallosupramolecular assemblies, which requires the use of the experimental formation constant of at least two complexes with different nuclearities for the parametrization of K_{inter} and K_{intra} [29]. Therefore, deviations from statistical repetitive binding can be only detected for multimetallic helicates, in which the number of metal ions is strictly larger than two (i.e. 'macrobicyclic' systems) as demonstrated with *Lehn's* helicates $[Cu_3(\mathbf{L3})_2]^{3+}$.

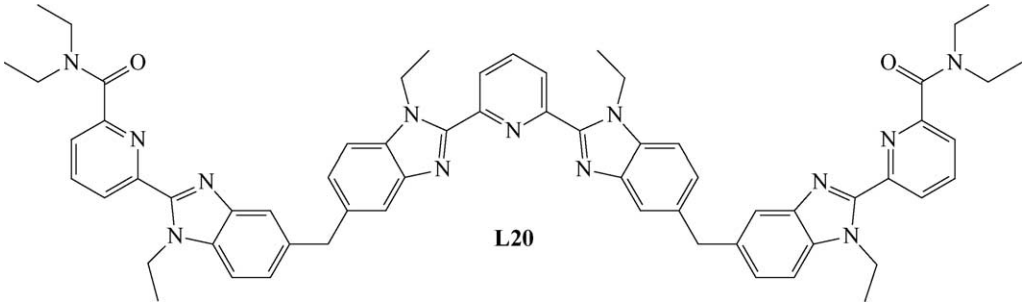

L20

The formation of the lanthanide-containing trimetallic triple-stranded helicates $[Ln_3(\mathbf{L20})_3]^{9+}$ (equilibria (27)–(28)) indeed fits this trimetallic criterion, but the thermodynamic experimental data are restricted to only two complexes with different nuclearities. This prevents the application of *Ercolani's* test for statistical repetitive binding [34].

$$2Ln^{3+} + 3\mathbf{L20} \rightleftharpoons [Ln_2(\mathbf{L20})_3]^{6+}, \quad \beta_{23}^{tri,LnLn} \quad (27)$$

$$3Ln^{3+} + 3\mathbf{L20} \rightleftharpoons [Ln_3(\mathbf{L20})_3]^{9+}, \quad \beta_{33}^{tri,LnLnLn} \qquad (28)$$

Original *Scatchard* plots computed with equilibria (27) and (28) in reference [34] suggested 'positive cooperativity', but a subsequent adequate analysis combining bi- and trimetallic analogous helicates eventually demonstrates that repetitive statistical binding occurs together with a strong negatively cooperative binding of the metal ions ($\Delta E_{intermetallic} \gg 0$) [35]. This thorough examination of the few systems for which reliable thermodynamic data have been reported, support *Ercolani's* conclusion, stated in our terminology, that positive deviation from statistical repetitive binding in artificial self-assembly systems is probably much more rare than it was previously thought [29]. However, the above-mentioned analyses of thermodynamic self-assemblies remains limited since (i) the affinity of the binding units along the strands must be identical (or at least very similar) and (ii) the intimate interaction parameters ΔE_{ij} measuring cooperativity cannot be obtained. For these reasons, sophisticated assemblies involving different binding units, such as trigonal bipyramids, grids, or catenates shown in Fig. 2 escape rationalization with the model of repetitive binding.

4. The intimate mechanism of helicate self-assembly: the kinetic approach

As often in this field, the ingenuity of Lehn and co-workers occupies a prominent position, and they first draw the attention of metallosupramolecular chemists on some unusual intermediates observed during the slow self-assembly kinetics of the pentametallic double-stranded helicates $[Cu_5(\mathbf{L5})_2]^{5+}$ [36]. ESI-MS data combined with NMR spectroscopy evidence the formation of hairpin-type intermediates which eventually self-assemble to give the final helicate (Fig. 11b) in strong contrast with the postulated linear mechanism (Fig. 11a).

From this striking observation, Albrecht-Gary and coworkers launched into a project aiming at the kinetic identification of the reaction pathways leading to double- and triple-stranded multimetallic helicates [37–40]. Firstly, the kinetic characteristics of the self-assembly of *Lehn's* trimetallic helicate $[Cu_3(\mathbf{L3})_2]^{3+}$ has been carefully investigated under pseudo-first order conditions. The complicated data can be satisfyingly fitted to the four-steps mechanism depicted in Fig. 12 [37]. Interestingly, the initial step corresponds to the fixation of two charged cations onto a single neutral strand, an unexpected behaviour, which can be tentatively assigned to (i) the limited charge borne by Cu(I) and (ii) the large distance between the two terminal bipyridine binding sites. Steps 2 and 3 correspond to the successive coordination of the second strand and the third metal, while the ultimate step deals with specific conformational changes leading to the thermodynamically stable entwined structure [37].

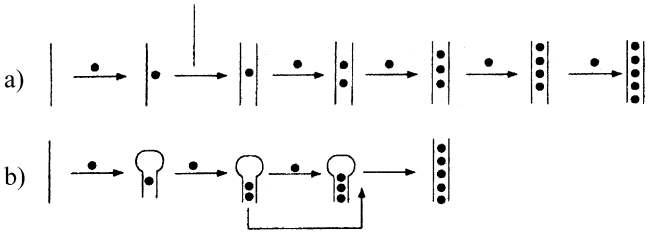

Fig. 11. Possible pathways for the formation of $[Cu_5(\mathbf{L5})_2]^{5+}$: (a) a linear successive mechanism, (b) a convergent mechanism with hairpin-type intermediates [36]. Reproduced with permission from [36], copyright VCH–Wiley, 1996.

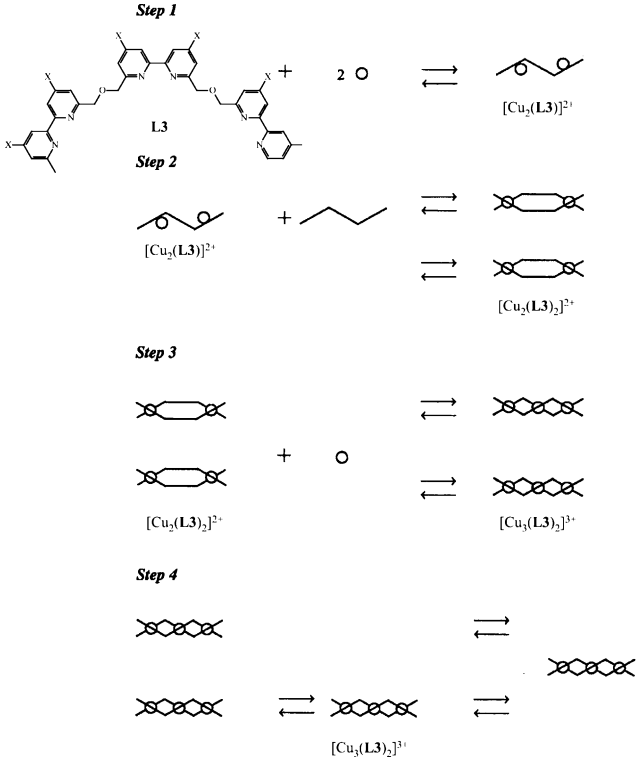

Fig. 12. Schematic representation of the mechanism of the self-asssembly of $[Cu_3(\mathbf{L3})_2]^{3+}$ [37]. Adapted from [37].

Closely related studies have been performed for elucidating the mechanism leading to the formation of the bimetallic triple-stranded helicates $[Fe_2(\mathbf{L21})_3]^{4+}$ (Fig. 13) [38], $[Eu_2(\mathbf{L22})_3]^{6+}$ (Fig. 14a) [39] and $[Eu_2(\mathbf{L23}\text{-}2H)_3]$ (Fig. 14b) [40].

Compared with the self-assembly of $[Cu_3(\mathbf{L3})_2]^{3+}$ (Fig. 12), the formation of the bimetallic triple-stranded helicates incorporates highly charged metal ions lying at close distance. This prevents the initial fixation of two cations onto a single neutral strand, and a second ligand is required with the Fe(II)/**L21** (Fig. 13) or Eu(III)/**L22** (Fig. 14a) systems to ensure that sufficient preorganization and partial charge compensation overcome the electrostatic repulsion. Depending on the initial stoichiometric conditions, the self-assembly provides different supramolecular edifices. In excess of lig-

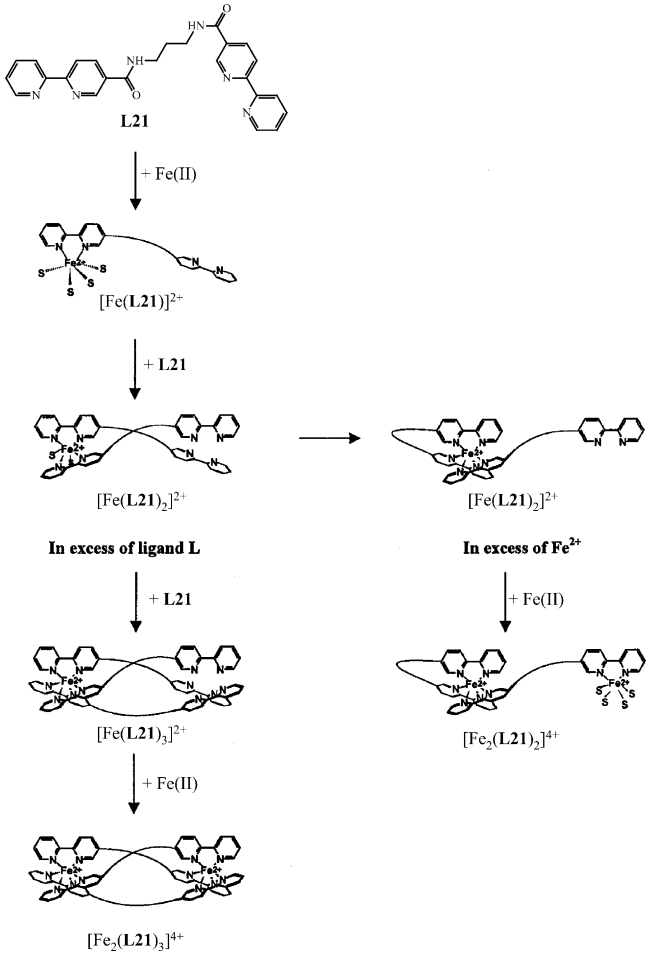

Fig. 13. Schematic representation of the mechanism of the self-asssembly of $[Fe_2(\mathbf{L21})_3]^{4+}$ [38]. Adapted from [38].

and, the expected triple-stranded helicates indeed correspond to the final complexes, but in excess of metal, the semi-hairpin $[Fe_2(\mathbf{L21})_2]^{4+}$ (Fig. 13) or the non-helical $[Eu_2(\mathbf{L22})_2]^{6+}$ (Fig. 14a) complexes are eventually obtained [38,39]. These observations definitely destroy the myth of the occurrence of self-assembly processes, in which the final programmed architectures is formed in one step whatever the external conditions. Moreover, the kinetic studies demonstrate that the fast organization of multicomponents edifices are strictly limited to specific stoichiometric ratios [39]. For instance, the use of an initial ratio Eu(III):**L22** = 2:3 rapidly leads to the thermodynamic equilibrium in which $[Eu_2(\mathbf{L22})_3]^{6+}$ is the major product (a few minutes for a total ligand concentration of 0.1 mM). However, the same reaction performed with a ratio of Eu(III):**L22** = 10:1 requires more than 1 h in order to reach chemical equilibrium [39]. The last ligand $[\mathbf{L23}\text{-}2H]^{2-}$ introduces charge neutralization as a novel parameter in helicate self-assembly. In these conditions, the coordination of a second metal to the initial intermediate $[Eu(\mathbf{L23}\text{-}2H)]^{+}$ competes with the fixation of a second ligand (Fig. 14b) [40]. This behaviour is reminiscent of that observed for the assembly of $[Cu_3(\mathbf{L3})_2]^{3+}$, which confirms that the intermetallic electrostatic repulsion is a crucial parameter for controlling the chemical pathway of the reaction. This latter aspect agrees with the systematic kinetic investigations performed by Crumbliss and coworkers on the decomposition mechanism of bimetallic $[Fe(III)_2\mathbf{L_3}]$ siderophores using natural (rhodotorullic) or synthetic dihydroxamic acids [41]. Although the flexibility of the spacers in these ligands provides variable structures for each of the 2:3, 2:2, 1:1, 1:3 intermediates, the stepwise fixation/decomplexation of charged metals and ligands systematically minimizes the intercomponent electrostatic factors, which are considered as the driving force for controlling the chemical pathways [41].

5. Toward predictive strategies in helicate self assembly: the site-binding model

Although the separation of intra- and intermolecular processes in *Ercolani*'s model is an efficient tool for rationalizing metallosupramolecular thermodynamic data, its predictive capacity is limited to the exploration of deviation from statistical repetitive binding for receptors possessing identical binding units. Moreover, no direct evaluation of the signs and magnitudes of the interaction parameters ΔE_{ij} is accessible. These limitations are particularly awkward for the formation of polymetallic complexes in which highly positively charged cations are expected to provide strong electrostatic effects which can be modulated by using ligand polarization and/or charge compensation as exemplified in the assembly of trivalent lanthanide helicates [42]. For addressing this challenge, Piguet and coworkers adapted the *site-binding* model for interpreting the thermodynamic data of lanthanide-containing triple-stranded helicates in which the three wrapped strands are considered as a preassembled one-dimensional receptors containing *n* adjacent coordination sites (Fig. 15) [43].

In this free energy model, an absolute affinity k_i is associated with the coordination site *i*, from which the free energy of complexation with a trivalent lanthanide Ln(III) can be obtained $\Delta G_i^{Ln} = -RT\ \ln(k_i^{Ln})$. A single free energy parameter ΔE_{ij} describes possible intermetallic interactions between adjacent metal ions lying in sites *i* and *j*. Application to the simple bimetallic triple-stranded helicate $[(Ln^1)_x(Ln^2)_{2-x}(\mathbf{L24})_3]^{6+}$ ($x = 0, 1, 2$, equilibrium (29)) [44] which contains two identical terminal (*t*) N_6O_3 sites (Fig. 15) leads to Eq. (30) for the total free energy of formation, whereby *s* is the degeneracy of the microscopic states [35]. In the latter equation, (i) the free energy cost associated with the preorganization of the three ligands in a triple-helical fashion to produce the box and (ii) the chiral factor $\delta = 2$ are neglected because they similarly affect the formation of any C_3- or D_3-symmetrical lanthanide complexes matching the *site-binding* model shown in Fig. 15. These contributions thus correspond to a fixed translation of the zero-level of the free energy scale,

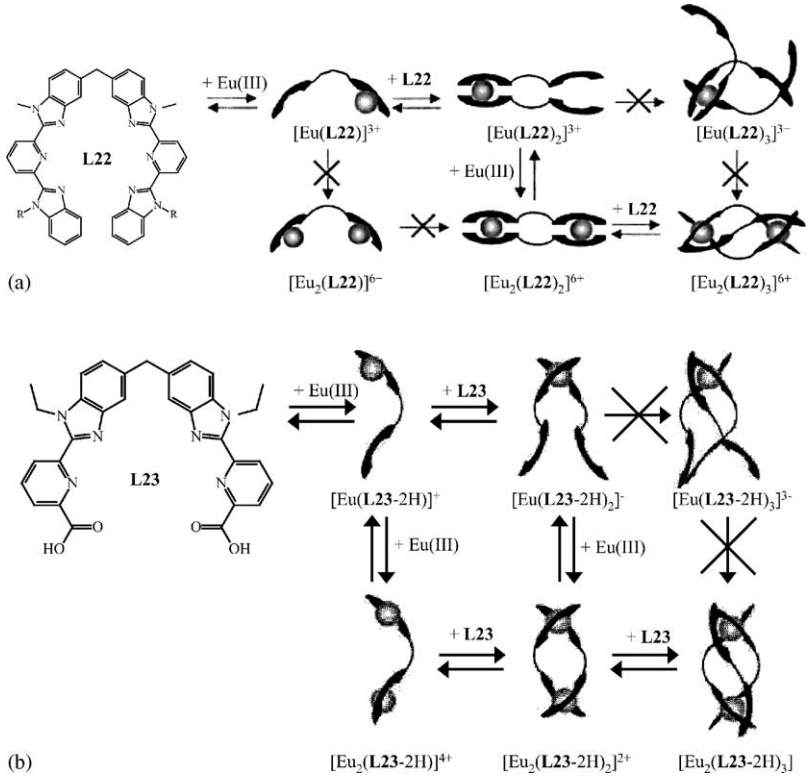

Fig. 14. Schematic representations of the mechanisms of the self-asssemblies of (a) $[Eu_2(\mathbf{L22})_3]^{6+}$ [39] and (b) $[Eu_2(\mathbf{L23}\text{-}2H)_3]$ [40]. Adapted from [39] and [40].

which is set to zero.

$$x[Ln^1]^{3+} + (2-x)[Ln^2]^{3+} + 3(\mathbf{L24}) \rightleftharpoons [(Ln^1)_x(Ln^2)_{2-x}(\mathbf{L24})_3]^{6+}, \quad \beta_{23}^{bi,Ln_x^1Ln_{2-x}^2} \tag{29}$$

$$\Delta G_{tot}([Ln_x^1Ln_{2-x}^2]) = -xRT\ \ln(k_t^{Ln^1}) - (2-x)RT \times \ln(k_t^{Ln^2}) + \Delta E_{Ln_x^1Ln_{2-x}^2} - RT\ \ln(s) = -RT\ \ln(\beta_{23}^{bi,Ln_x^1Ln_{2-x}^2}) \tag{30}$$

A straightforward mathematical transformation leads to Eq. (31) assuming that the intermetallic interaction parameter is expressed as the Boltzmann factor $u_{Ln_x^1Ln_{2-x}^2} = e^{-\left(\Delta E_{Ln_x^1Ln_{2-x}^2}/RT\right)}$.

$$\beta_{23}^{bi,Ln_x^1Ln_{2-x}^2} = s(k_t^{Ln^1})(k_t^{Ln^2})^{2-x}u_{Ln_x^1Ln_{2-x}^2} \tag{31}$$

The latter equation correlates the experimentally accessible macroscopic formation constants for the triple-stranded helical complexes matching the *site-binding* model with simple parameters, which reflects specific affinities (k_i) and intermetallic interactions (u_{ij}). Since this free energy model does not includes the free energy change asssociated with the preassembly of the triple-stranded receptor, the absolute values of k_i, and the associated free energy terms must be interpreted with caution. However, comparisons between different sites in the same assembly remain fully justified. On the other hand, u_{ij} (i.e. ΔE_{ij}) is a direct measure of the influence of the fixation of one metal onto the neighbouring sites for further complexation processes. When u_{ij} = 1 (i.e. ΔE_{ij} = 0), the fixation of the first cation has no influence on the next complexation processes. This corresponds to the concept of non-cooperativity [26]. When u_{ij} < 1 (i.e. ΔE_{ij} > 0) or u_{ij} > 1 (i.e. ΔE_{ij} < 0), the fixation of the first metal, respectively, hinders or favors the coordination of a metal in the neighbouring site, in line with negative or positive cooperativity. The thorough investigation of the strict self-assembly leading to $[Ln_2(\mathbf{L24})_3]^{6+}$ demonstrates the formation of the intermediate C_3-symmetrical complex $[Ln(\mathbf{L24})_3]^{3+}$ existing in solution exclusively as the facial (i.e. HHH) isomer (equilibrium (32)). This structure exactly fits the *site-binding* model in which a single site is occupied (Fig. 15) and, for each pair of lanthanide Ln^1/Ln^2, equilibria (29) and (32) provide five experimental macroscopic constants which can be modelled with Eqs. (33)–(37) by using five parameters $k_t^{Ln^1}$, $k_t^{Ln^2}$, $u_{Ln^1Ln^1}$, $u_{Ln^2Ln^2}$ and $u_{Ln^1Ln^2}$ [35].

$$Ln^{3+} + 3\mathbf{L24} \rightleftharpoons fac - [Ln(\mathbf{L24})_3]^{3+}, \quad \beta_{13}^{bi,Ln} \tag{32}$$

$$\beta_{23}^{bi,Ln^1Ln^1} = \left(k_t^{Ln^1}\right)^2 u_{Ln^1Ln^1} \tag{33}$$

$$\beta_{23}^{bi,Ln^2Ln^2} = \left(k_t^{Ln^2}\right)^2 u_{Ln^2Ln^2} \tag{34}$$

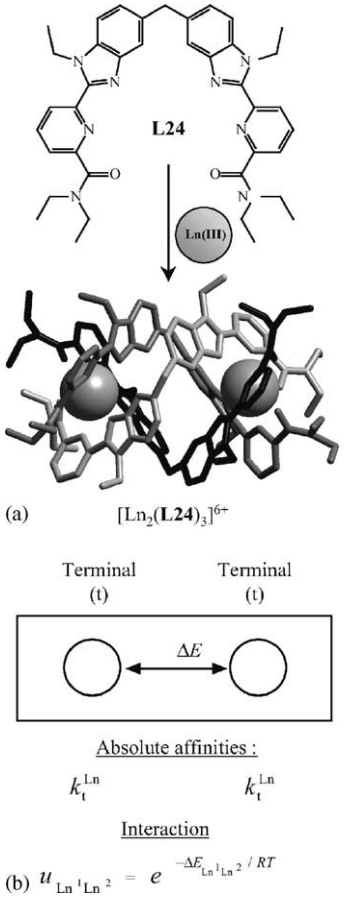

Fig. 15. (a) Formation and solution structure of $[Ln_2(\mathbf{L24})_3]^{6+}$ and (b) associated thermodynamic *site-binding* model [35].

$$\beta_{23}^{bi,Ln^1Ln^2} = 2\left(k_t^{Ln^1}\right)\left(k_t^{Ln^2}\right)u_{Ln^1Ln^2} \quad (35)$$

$$\beta_{13}^{bi,Ln^1} = 2\left(k_t^{Ln^1}\right) \quad (36)$$

$$\beta_{13}^{bi,Ln^2} = 2\left(k_t^{Ln^2}\right) \quad (37)$$

Interestingly, the thermodynamic exchange constant which correlates homo- and heterobimetallic helicates (equilibrium (38)) does not significantly deviates from $K_{exch} = 4$, a statistical value which implies that the interaction parameters are identical within experimental error for any pairs of lanthanides coordinated in the two adjacent sites ($\Delta E_{Ln^1Ln^1} = \Delta E_{Ln^2Ln^2} = \Delta E_{Ln^1Ln^2}$) [35]. This implies that the fixation of any Ln^1 has the same influence on the coordination of any other Ln^2, which is diagnostic for the absence of allosteric effect.

$$[(Ln^1)_2(\mathbf{L24})_3]^{6+} + [(Ln^2)_2(\mathbf{L24})_3]^{6+} \rightleftharpoons 2[(Ln^1)(Ln^2)(\mathbf{L24})_3]^{6+}, \quad K_{exch} \quad (38)$$

The number of parameters is reduced to three ($k_t^{Ln^1}$, $k_t^{Ln^2}$, u) and least-squares fits for 21 different pairs gives $\log(k_t^{Ln})$, which exhibit a slightly concave dependence along the lanthanide series (Fig. 16a), together with free energy interactions parameters varying around an average value of $\bar{\Delta E}$ = 51(7) kJ mol^{-1} (Fig. 16b) [35]. The positive value of ΔE unambigously demonstrates that the intermetallic interaction in $[Ln^1Ln^2(\mathbf{L24})_3]^{6+}$ is repulsive in agreement with simple electrostatic considerations, which leads to ΔE = 48 kJ mol^{-1} for the work required for approaching two triply charged cation at ca. 9.1 Å in acetonitrile (dielectric constant $\varepsilon_r \approx 30$) [35].

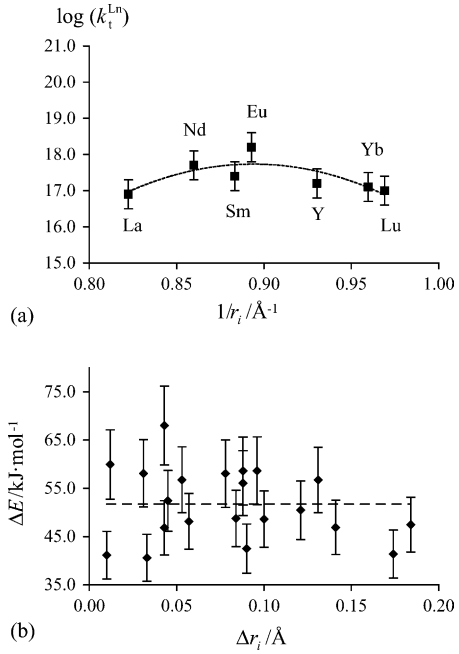

Fig. 16. (a) Computed absolute affinities for the terminal sites ($\log(k_t^{Ln})$) as a function of the inverse of nine-coordinate ionic radii and (b) intermetallic interaction parameters (ΔE) in the triple-stranded bimetallic helicates $[Ln_2(\mathbf{L24})_3]^{6+}$ as a function of $\Delta r_i = |r_{Ln^1} - r_{Ln^2}|$. Adapted from reference [35].

Reference [35] concludes that (i) negative cooperativity operates and (ii) no specific intermetallic recognition occurs since $\Delta E_{Ln^1Ln^1} = \Delta E_{Ln^2Ln^2} = \Delta E_{Ln^1Ln^2}$. It is noteworthy, that this model is predictive since (i) the study of the assembly of the homobimetallic helicates $[(Ln^1)_2(\mathbf{L24})_3]^{6+}$ and $[(Ln^2)_2(\mathbf{L24})_3]^{6+}$ allows the prediction of the stability constant for the parent heterobimetallic helicate $[(Ln^1)(Ln^2)(\mathbf{L24})_3]^{6+}$ and (ii) the study of two different pairs Ln^1/Ln^2 and Ln^1/Ln^3 allows the calculation of stability constants for the Ln^2/Ln^3 system. The lack of Ln-dependent interactions in $[(Ln^1)_x(Ln^2)_{2-x}(\mathbf{L24})_3]^{6+}$ (i.e. $u_{Ln^1Ln^1} = u_{Ln^2Ln^2} = u_{Ln^1Ln^2}$) requires the introduction of different binding units along the ligand strand displaying specific absolute affinities for the selective preparation of heterobimetallic f–f′ helicates. The unsymmetrical heterotopic bis-tridentate ligand **L15** matches this criterion since a N_3 segment is connected to a N_2O binding unit (Fig. 7) [19]. However, the unavoidable HHH↔HHT isomerism in $[Ln_2(\mathbf{L15})_3]^{6+}$ produces two different helicates, each possessing two different coordination sites with specific affinities for the metal ions. Therefore, four different absolute affinities

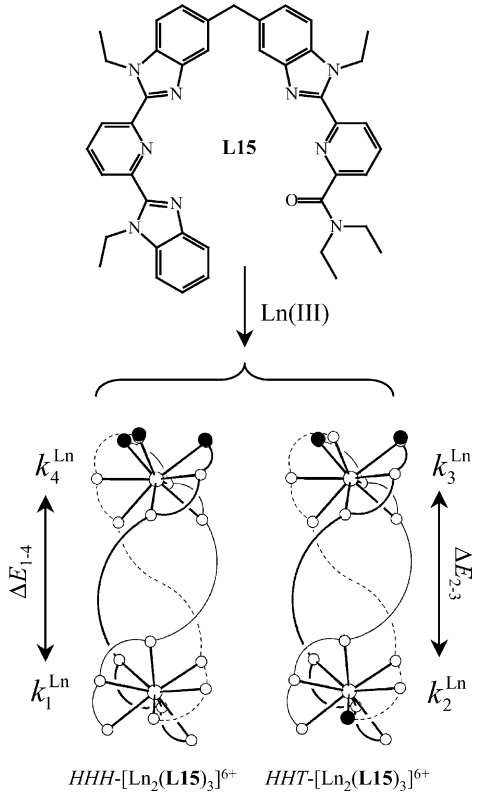

Fig. 17. Isomerism in the self-assembly of $[Ln_2(\mathbf{L15})_3]^{6+}$ and associated *site-binding* models: (●) O-donor and (◯) N-donor group.

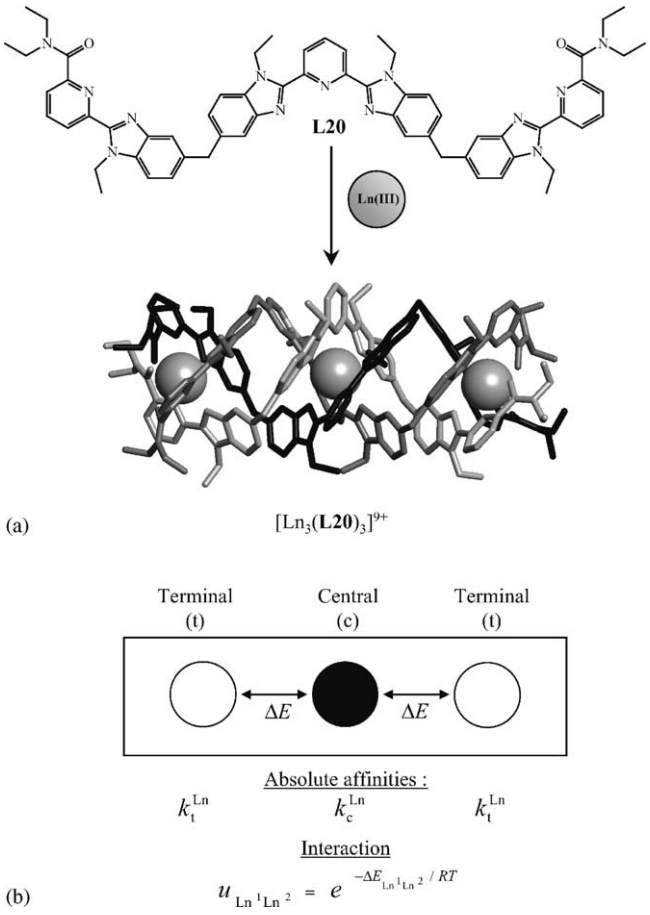

Fig. 18. (a) Formation and solution structure of $[Ln_3(\mathbf{L20})_3]^{9+}$ and (b) associated thermodynamic *site-binding* model [43].

k_1^{Ln} (N_9), k_2^{Ln} (N_8O), k_3^{Ln} (N_7O_2) and k_4^{Ln} (N_6O_3) and two intermetallic interaction parameters ΔE_{1-4} and ΔE_{2-3} are required for the microscopic modelling of the two complexes HHH-$[Ln_2(\mathbf{L15})_3]^{6+}$ and HHT-$[Ln_2(\mathbf{L15})_3]^{6+}$ (Fig. 17). It becomes apparent that the number of required parameters exceeds the amount of experimental macroscopic constants. It is thus necessary to limit the description of the assembly process to macroscopic constants including different conformations, in which the above parameters k_1^{Ln} (N_9), k_2^{Ln} (N_8O), k_3^{Ln} (N_7O_2) and k_4^{Ln} (N_6O_3) are not easily accessible.

A high symmetry in the final helicates combined with the absence of isomerism significantly reduces the number of parameters. The C_{2v}-symmetrical ligand **L20** has been designed for this purpose because the associated trimetallic helicates $[Ln_3(\mathbf{L20})_3]^{9+}$ evidence D_3-symmetry (Fig. 18) [34,42].

The intercalation of the central (c) N_9 site between the two terminal (t) N_6O_3 sites (Fig. 18) complicates the expression of the total free energy for the formation of $[(Ln^1)_x(Ln^2)_{3-x}(\mathbf{L20})_3]^{9+}$ (x = 0, 1, 2, 3). Application of the *site-binding* model to equilibrium (39) leads to Eq. (40) for the calculation of each microscopic constant [43]. Note that a microscopic constant depends on the exact position of each metal ion in the different sites (Eqs. (43)–(48)), while a macroscopic constant combines the different microscopic constants corresponding to the same stoichiometry.

$$x[Ln^1]^{3+} + (3-x)[Ln^2]^{3+} + 3\mathbf{L20} \rightleftharpoons [(Ln^1)_x(Ln^2)_{3-x}(\mathbf{L20})_3]^{9+}, \quad \beta_{33}^{tri,Ln_x^1Ln_{3-x}^2} \tag{39}$$

$$\begin{aligned}\Delta G_{tot}[Ln_x^1Ln_{3-x}^2] &= -s_c^{Ln^1} RT \\ &\times \ln(k_c^{Ln^1}) - s_t^{Ln^1} RT \ln(k_t^{Ln^1}) \\ &- s_c^{Ln^2} RT \ln(k_c^{Ln^2}) - s_t^{Ln^2} RT \ln(k_t^{Ln^2}) \\ &+ (s_c^{Ln^1} s_t^{Ln^1}) \Delta E_{Ln^1Ln^1} + (s_c^{Ln^2} s_t^{Ln^2}) \Delta E_{Ln^2Ln^2} \\ &+ (s_c^{Ln^1} s_t^{Ln^2} + s_c^{Ln^2} s_t^{Ln^1}) \Delta E_{Ln^1Ln^2} \\ &- RT, \ln(s) = -RT \ln(\beta_{33}^{tri,Ln_x^1Ln_{3-x}^2})\end{aligned} \tag{40}$$

where s^{Ln^i} and $s_t^{Ln^i}$ are state variables which correspond to the number of lanthanide i occupying the central, respectively, the terminal sites (for instance, the complex $[(Ln^1)(Ln^1)(Ln^2)(\mathbf{L20})_3]^{9+}$ possesses $s_c^{Ln^1} = 1$, $s_t^{Ln^1} = 1$, $s_c^{Ln^2} = 0$ and $s_t^{Ln^2} = 1$, while $[(\mathbf{Ln}^2)_3(\mathbf{L20})_3]^{9+}$ is characterized by $s_c^{Ln^1} = 0$, $s_t^{Ln^1} = 0$, $s_c^{Ln^2} = 1$ and $s_t^{Ln^2} = 2$). Again,

a straightforward mathematical transformation leads to Eq. (41) assuming that the interaction parameter is expressed as the Boltzmann factor $u_{\mathrm{Ln}^i\mathrm{Ln}^j} = \mathrm{e}^{-(\Delta E_{\mathrm{Ln}^i\mathrm{Ln}^j}/RT)}$.

$$\beta_{33}^{\mathrm{tri,Ln}_x^1\mathrm{Ln}_{3-x}^2} = s(k_c^{\mathrm{Ln}^1})^{s_c^{\mathrm{Ln}^1}}(k_t^{\mathrm{Ln}^1})^{s_t^{\mathrm{Ln}^1}}(k_c^{\mathrm{Ln}^2})^{s_c^{\mathrm{Ln}^2}}(k_t^{\mathrm{Ln}^2})^{s_t^{\mathrm{Ln}^2}} \times (u_{\mathrm{Ln}^1\mathrm{Ln}^1})^{(s_c^{\mathrm{Ln}^1}s_t^{\mathrm{Ln}^1})}(u_{\mathrm{Ln}^2\mathrm{Ln}^2})^{(s_c^{\mathrm{Ln}^2}s_t^{\mathrm{Ln}^2})} \times (u_{\mathrm{Ln}^1\mathrm{Ln}^2})^{(s_c^{\mathrm{Ln}^1}s_t^{\mathrm{Ln}^2}+s_c^{\mathrm{Ln}^2}s_t^{\mathrm{Ln}^1})} \quad (41)$$

The thorough study of the assembly process by spectrophotometry, ESI-MS and NMR spectroscopies reveals the existence of $[\mathrm{Ln}_2(\mathbf{L20})_3]^{6+}$ as a thermodynamic intermediate (equilibrium (42)) [34]. However, the shift of one ligand in $[\mathrm{Ln}_2(\mathbf{L20})_3]^{6+}$ with respect to the two other strands according to the 'vernier' mechanism [11b], produces an unsaturated complex, in which only two neighbouring nine-coordinate sites are available for complexation [35]. Its structure does not fit the *site-binding* model and $\beta_{23}^{\mathrm{tri,Ln}}$ cannot be used for extracting absolute affinites and interaction parameters.

$$2\mathrm{Ln}^{3+} + 3\mathbf{L20} \rightleftharpoons [\mathrm{Ln}_2(\mathbf{L20})_3]^{6+}, \quad \beta_{23}^{\mathrm{tri,Ln}} \quad (42)$$

Therefore, only six microscopic constants (Eqs. (43)–(48)), of which five are mathematically independent, can be considered for fitting the five parameters $k_t^{\mathrm{Ln}^1}$, $k_t^{\mathrm{Ln}^2}$, $k_c^{\mathrm{Ln}^1}$, $k_c^{\mathrm{Ln}^2}$ and u required for modelling each $\mathrm{Ln}^1/\mathrm{Ln}^2$ pair (it is assumed that $u_{\mathrm{Ln}^1\mathrm{Ln}^1} = u_{\mathrm{Ln}^2\mathrm{Ln}^2} = u_{\mathrm{Ln}^1\mathrm{Ln}^2}$) [43]. Moreover, each equation is modulated by the square of the Boltzmann parameter (u^2), which prevents its independent determination [43]. Its value is thus arbitrarily fixed to $u = 1$ (i.e. $\Delta E = 0$), and the fitted $\log(k_t^{\mathrm{Ln}})$ and $\log(k_c^{\mathrm{Ln}})$ are depicted in Fig. 19 [43]. Note that these six microscopic constants may be combined to give four macroscopic constants corresponding to $\beta_{33}^{\mathrm{tri,Ln}^1\mathrm{Ln}^1\mathrm{Ln}^1}$, $\beta_{33}^{\mathrm{tri,Ln}^2\mathrm{Ln}^2\mathrm{Ln}^2}$, $\beta_{33}^{\mathrm{tri,Ln}^1\mathrm{Ln}^1\mathrm{Ln}^2} + \beta_{33}^{\mathrm{tri,Ln}^1\mathrm{Ln}^2\mathrm{Ln}^1}$ and $\beta_{33}^{\mathrm{tri,Ln}^1\mathrm{Ln}^2\mathrm{Ln}^2} + \beta_{33}^{\mathrm{tri,Ln}^2\mathrm{Ln}^1\mathrm{Ln}^2}$.

$$\beta_{33}^{\mathrm{tri,Ln}^1\mathrm{Ln}^1\mathrm{Ln}^1} = (k_t^{\mathrm{Ln}^1})^2(k_c^{\mathrm{Ln}^1})(u_{\mathrm{Ln}^1\mathrm{Ln}^1})^2 \quad (43)$$

$$\beta_{33}^{\mathrm{tri,Ln}^1\mathrm{Ln}^1\mathrm{Ln}^2} = 2(k_t^{\mathrm{Ln}^1})(k_c^{\mathrm{Ln}^1})(k_t^{\mathrm{Ln}^2})u_{\mathrm{Ln}^1\mathrm{Ln}^1}u_{\mathrm{Ln}^1\mathrm{Ln}^2} \quad (44)$$

$$\beta_{33}^{\mathrm{tri,Ln}^1\mathrm{Ln}^2\mathrm{Ln}^1} = (k_t^{\mathrm{Ln}^1})^2(k_c^{\mathrm{Ln}^2})(u_{\mathrm{Ln}^1\mathrm{Ln}^2})^2 \quad (45)$$

$$\beta_{33}^{\mathrm{tri,Ln}^1\mathrm{Ln}^2\mathrm{Ln}^2} = 2(k_t^{\mathrm{Ln}^1})(k_c^{\mathrm{Ln}^2})(k_t^{\mathrm{Ln}^2})u_{\mathrm{Ln}^1\mathrm{Ln}^2}u_{\mathrm{Ln}^2\mathrm{Ln}^2} \quad (46)$$

$$\beta_{33}^{\mathrm{tri,Ln}^2\mathrm{Ln}^1\mathrm{Ln}^2} = (k_t^{\mathrm{Ln}^2})^2(k_c^{\mathrm{Ln}^1})(u_{\mathrm{Ln}^1\mathrm{Ln}^2})^2 \quad (47)$$

$$\beta_{33}^{\mathrm{tri,Ln}^2\mathrm{Ln}^2\mathrm{Ln}^2} = (k_t^{\mathrm{Ln}^2})^2(k_c^{\mathrm{Ln}^2})(u_{\mathrm{Ln}^2\mathrm{Ln}^2})^2 \quad (48)$$

The concave bowl-shape curve obtained along the lanthanide series for the terminal N_6O_3 site (Fig. 19a) agrees with that previously found for the same site in the bimetallic analogue $[\mathrm{Ln}_2(\mathbf{L24})_3]^{6+}$ (Fig. 16a), although their absolute magnitudes cannot be compared because the interaction parameter ΔE for the trimetallic helicates is fixed to zero. The inverted electrostatic trend found

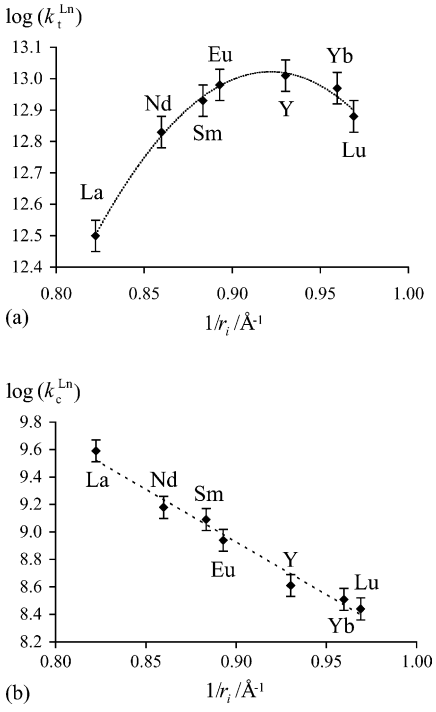

Fig. 19. Computed absolute affinities for (a) the terminal sites ($\log(k_t^{\mathrm{Ln}})$) and (b) the central site ($\log(k_c^{\mathrm{Ln}})$) in the triple-stranded trimetallic helicates $[\mathrm{Ln}_3(\mathbf{L20})_3]^{9+}$ as a function of the inverse of nine-coordinate ionic radii. The interaction parameter ΔE is arbitrarily set to zero (see text) [43].

for the central N_9 site (Fig. 19b) is remarkable, and it closely matches related data collected for the monometallic model complexes [Ln(2,6-bis(1-methyl-benzimidazol-2yl)pyridine)$_3$]$^{3+}$, which possess identical N_9 sites [45]. One important question remains unsolved: does the absolute affinity of the terminal metallic N_6O_3 sites (k_t^{Ln}) and the interaction parameter (u) vary when the nuclearity increases on going from in $[\mathrm{Ln}_2(\mathbf{L24})_3]^{6+}$ to $[\mathrm{Ln}_3(\mathbf{L20})_3]^{9+}$? This point can be addressed by fitting Eqs. (43)–(48) for the trimetallic helicates $[\mathrm{Ln}_3(\mathbf{L20})_3]^{9+}$, and by using the interaction parameter found for $[\mathrm{Ln}_2(\mathbf{L24})_3]^{6+}$ ($\Delta E = 51\,\mathrm{kJ\,mol^{-1}}$). The resulting absolute affinities of the terminal metallic N_6O_3 sites (k_t^{Ln}) in the trimetallic complexes $[\mathrm{Ln}_3(\mathbf{L20})_3]^{9+}$ indeed closely match those found for $[\mathrm{Ln}_2(\mathbf{L24})_3]^{6+}$ (Eqs. (33)–(37)), which implies that a single k_t^{Ln} is required for both complexes. In other words: (i) the successive formation of bimetallic and trimetallic helicates obeys statistical repetitive binding, and (ii) the formal free energies required for the preassembly of the D_3-symmetrical receptors $[\mathbf{L20}]_3$ and $[\mathbf{L24}]_3$ are similar.

This assumption can be confirmed by applying *Ercolani*'s model (Eq. (8)) [29] to the equilibria (29) and (32). Eqs. (49) and (50) result, from which $K_{\mathrm{inter}}^{\mathrm{Ln}}$ and $K_{\mathrm{intra}}^{\mathrm{Ln}}$ can be easily calculated for each lanthanide along the series [35].

$$\beta_{13}^{\mathrm{bi,Ln}} = \delta\sigma_{\mathrm{facial}}(K_{\mathrm{inter}}^{\mathrm{Ln}})^3 \quad (49)$$

$$\beta_{23}^{\mathrm{bi,LnLn}} = \delta\sigma_{\mathrm{sa}}(K_{\mathrm{inter}}^{\mathrm{Ln}})^4(K_{\mathrm{intra}}^{\mathrm{Ln}})^2 \quad (50)$$

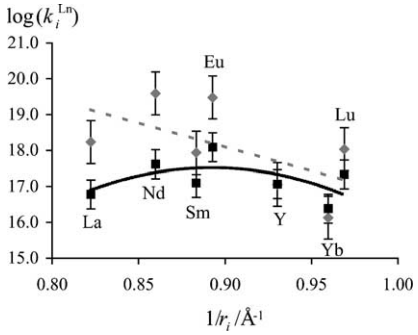

Fig. 20. Computed absolute affinities for the terminal sites ($\log(k_t^{Ln})$, black) and the central site ($\log(k_c^{Ln})$, grey) in the triple-stranded bimetallic $[Ln_2(\mathbf{L24})_3]^{6+}$ and trimetallic $[Ln_3(\mathbf{L20})_3]^{9+}$ helicates as a function of the inverse of nine-coordinate ionic radii [35].

Assuming that the affinity of the terminal N_6O_3 site is comparable to that of the central N_9 site in $[Ln_3(\mathbf{L20})_3]^{9+}$, the statistical formation constant for $[Ln_3(\mathbf{L20})_3]^{9+}$ can be estimated with Eq. (51) [29,35].

$$\beta_{33}^{tri,stat} = \delta\sigma_{sa}(K_{inter}^{Ln})^5(K_{intra}^{Ln})^4 \quad (51)$$

As expected, the calculated constants $\beta_{33}^{tri,stat}$ indeed closely reproduce the experimental data $\beta_{33}^{tri,LnLnLn}$, in line with (i) a rough invariance of k_t^{Ln} and ΔE when going from $[Ln_2(\mathbf{L24})_3]^{6+}$ to $[Ln_3(\mathbf{L20})_3]^{9+}$ and (ii) similar free energy cost for the preorganization of the three strands in these complexes [35]. Therefore, a global least-square treatment considering Eqs. (33)–(37) and Eqs. (43)–(48) (a total of 11 equations) significantly improves the physical significance of the fitting process for the five parameters $k_t^{Ln^1}$, $k_t^{Ln^2}$, $k_c^{Ln^2}$, $k_c^{Ln^2}$ and u (Fig. 20). The trends in $\log(k_t^{Ln})$ and $\log(k_c^{Ln})$ are confirmed (Fig. 20) while the final average interaction parameter $\overline{\Delta E} = 51(6)\,kJ\,mol^{-1}$ points to strongly negative cooperativity. Again, the invariance of ΔE for any Ln^1/Ln^2 pair is disappointing for the rational programming of heterometallic f–f′ helicates, but the existence of two sites with different affinities along the lanthanide series in $[Ln_3(\mathbf{L20})_3]^{9+}$ may be judiciously exploited for overcoming this limitation. For instance, the mixing of La(III):Eu(III):**L20** in a 1:2:3 ratio ($[\mathbf{L20}]_{tot} = 10^{-2}\,mol\,dm^{-3}$) results in the formation of 50% of $[EuLaEu(\mathbf{L20})_3]^{9+}$. This value represents a considerable deviation from the binomial statistical distribution, which predicts the formation of only 14% of this complex if the three sites are equivalent [43].

This combination of *Ercolani*'s and *site-binding* thermodynamic models appears particularly efficient for the thorough interpretation of other monodimensional assemblies. Let us recall the above application of *Ercolani*'s model (Section 3) for the evaluation of the statistical factor $K_2/K_1 = 0.25$, for which non-cooperativity occurs in the formation of $[Fe(\mathbf{L}i)]$ and $[Fe_2(\mathbf{L}i)]$, assuming that the two sites are equivalent ($i = 17, 18$; equilibria (5) and (6)). The application of the *site-binding* model is identical to that described in Fig. 15b, and β_{11} (equilibrium (5)) and β_{21} (equilibrium (9)) are given by Eqs. (52) and (53), which are very similar to Eqs. (10) and (11), except for the introduction of the interaction parameter u.

$$\beta_{11}^{Li} = 2k_t^{Li} \quad (52)$$

$$\beta_{21}^{Li} = (k_t^{Li})^2 u^{Li} \quad (53)$$

Taking into account the experimental value reported for β_{11} and β_{21} for **L17** and **L18** [32b], we calculated that $\log(k_t^{L17}) = \log(K_{inter}^{L17}) = 5.52$ and $\Delta E_{intermetallic}(\mathbf{L17}) = -2.7\,kJ\,mol^{-1}$ (i.e. positive cooperativity), and $\log(k_t^{L18}) = \log(K_{inter}^{L18}) = 6.45$ and $\Delta E_{intermetallic}(\mathbf{L18}) = 0.2 \approx 0\,kJ\,mol^{-1}$ (i.e. no cooperativity). We conclude that for a pure intermolecular process, the two models converge to give a single description similar to that originally used in the protein/ligand model. However, this correlation is less obvious when inter- and intramolecular processes are involved in multicomponents assemblies (compare Eqs. (33) and (36) (*site-binding* model) with Eqs. (49) and (50) (*Ercolani*'s model)), and it becomes irreconcilable when different affinities are assigned to the different binding sites because *Ercolani*'s model becomes inadequate. Finally, the systematic application of these two complementary approaches may bring some light onto the thermodynamic parameters controlling successive steps in complicated chemical pathways. For instance, the formation of $[Eu_2(\mathbf{L23}\text{-}2H)_3]$ depicted in Fig. 14b [40] contains valuable thermodynamic information dealing with the effect of charge compensation on the successive fixation of trivalent lanthanide ions. The thermodynamic stability constants associated with equilibria (54)–(56) can be derived from the kinetic data [40].

$$[\mathbf{L23} - 2H]^{2-} + Eu^{3+} \rightleftharpoons [Eu(\mathbf{L23}\text{-}2H)]^{+},\quad K_1 = \beta_{11} = 1.9(5) \times 10^4 \quad (54)$$

$$[Eu(\mathbf{L23}\text{-}2H)]^{+} + Eu^{3+} \rightleftharpoons [Eu_2(\mathbf{L23}\text{-}2H)]^{4+},\quad K_2 = 1.2(6) \times 10^2 \quad (55)$$

$$[\mathbf{L23}\text{-}2H]^{2-} + 2Eu^{3+} \rightleftharpoons [Eu_2(\mathbf{L23}\text{-}2H)]^{4+},\quad \beta_{21} = 2.3(1.3) \times 10^6 \quad (56)$$

According to a chemical point of view, equilibria (54) and (55) are strictly equivalent to equilibria (5) and (9), and thus strictly correspond to two successive intermolecular processes. We thus expect the same statistical factor $K_2/K_1 = 0.25$ in absence of interaction ($\Delta E = 0$). The experimental ratio amounts to $(K_2/K_1)_{exp} = 6(4) \times 10^{-3}$ which implies negative cooperativity despite partial charge neutralization brought by the negative ligand strand. Obviously, Eqs. (52) and (53) also hold for analyzing equilibria (54) and (56), and we obtain $\log(k_t^{L23}) = 3.98$ and $\Delta E_{intermetallic}(\mathbf{L23}) = 9.1\,kJ\,mol^{-1}$. We notice however, that the intermetallic repulsion param-

eter in $[Eu_2(\mathbf{L23}\text{-}2H)]^{4+}$ (9.1 kJ mol^{-1}) is significantly reduced, when compared with that found for $[Eu_2(\mathbf{L24})_3]^{6+}$ (51 kJ mol^{-1}). Since both ion are held at ca. 9 Å in these molecular edifices, we can ascribe this decrease to a combination of (i) the dielectric constants of the medium separating the point charges (water for $[Eu_2(\mathbf{L23}\text{-}2H)]^{4+}$ ($\varepsilon_r \approx 80$) and acetonitrile for $[Eu_2(\mathbf{L24})_3]^{6+}$ ($\varepsilon_r \approx 30$)) [41], and (ii) the reduced charge resulting from complexation of Eu^{3+} to terminal negative carboxylates in $[Eu_2(\mathbf{L23}\text{-}2H)]^{4+}$. A simple electrostatic model considering two doubly-charged cations held at 9 Å in water provides a repulsion parameter of 7.9 kJ mol^{-1}, in satisfying agreement with the experimental data found for $[Eu_2(\mathbf{L23}\text{-}2H)]^{4+}$.

6. From helicates to multimetallic supramolecular architectures

6.1. Infinite one-dimensional metallo-organic polymers

Consider now a long linear receptor with a large number of sites. An important situation is where the receptor has binding sites, which are either empty or can bind a metal ion, as indicated in Fig. 10. Another situation is encountered when all the sites of the receptor are saturated with one type of metal ion and these metal ions can be exchanged for a different type. This situation has been discussed for the bi- and trimetallic helicates (see Section 5). Evidently, it should be possible to generalize the above treatment proposed for the receptor with two and three sites to a receptor with an arbitrary number of sites. Eventually, the interesting question arises what happens when the receptor is very long, in other words in the limit of an infinite number of sites.

This fundamental problem has received substantial attention in the past, but hardly in the context of coordination chemistry [30]. For this reason, a brief discussion of the situation is given here. The problem has been amply treated within the statistical mechanics community, and is referred to as the Ising model. The key application of this model in the context of ion binding to a receptor is the acid–base titration of a weak polyelectrolyte, as originally suggested by Steiner [46] and Marcus [47]. In the meantime, the model was generalized and applied to various linear polyamines [48,49] and polycarboxylates [50,51]. The polyelectrolyte represents the linear receptor and the ionizable groups the sites for binding the protons. The same model is equally applicable to the binding of metal ions to a linear receptor. Here we focus on a very long receptor with an infinite number of sites. In practice, this limit is reached relatively soon, typically with 10–20 sites.

The free energy of the receptor (ΔG) depends on the occupation state of the individual binding sites. Each site can be either empty, or occupied with a bound metal ion. For this reason one introduces the state variable s_i, which is $s_i = 0$ when the site is empty, and $s_i = 1$ when occupied (see Eq. (40) for an example). With these variables, the free energy of one mole of identical receptors with N sites can be written in the following form, namely

$$\Delta G = -\mu \sum_{i=1}^{N} s_i + \Delta E \sum_{i=1}^{N-1} s_i s_{i+1} \tag{57}$$

The first term corresponds to the free energy contribution of the binding of the metal ions to the sites, and the second term corresponds to interactions between the sites. Each pair of neighbouring metal ions interacts with the free energy ΔE, this contribution enters the free energy only when two neighbouring sites are occupied. Further above, we have used the notation $\mu = RT \ln K$, where K is the binding constant of a metal ion to the receptor, T the absolute temperature, and R is the gas constant.

Since the system consists of a large number of sites (whose number will be finally considered to be infinite) a description in terms of complexation constants is not practicable. The larger the receptor, the more microstates have to be considered, leading to progressively increasing number of binding constants. In the limit of infinite number of sites, an infinite number of constants would have to be considered. On the other hand, the binding isotherm is always well-defined and can be obtained in a straightforward fashion. For this calculation one has to evaluate the partition function

$$\Xi = \sum_{s_1=0,1} \sum_{s_2=0,1} \cdots \sum_{s_N=0,1} a^n \, \mathrm{e}^{-\Delta G/RT} \tag{58}$$

where the free energy is given by Eq. (57), a is the activity of metal ion, and $n = \sum_{i=1}^{N} s_i$ is the number of ions bound to the receptor. The sum runs over all possible microstates of the chain. Several established techniques are available to evaluate sums of this type partition functions, for example, the transfer matrix method. In the long chain limit, the partition function Ξ can be evaluated explicitly as λ^N in which λ corresponds to the largest eigenvalue of the transfer matrix (Eq. (59)) [30].

$$\lambda = \frac{1 + zu}{2 + \sqrt{z + (1 + zu)^2/2}} \tag{59}$$

where z the Ka and $u = \mathrm{e}^{-\Delta E/kT}$. Once the partition function is known, the fractional degree of occupancy (adsorption isotherm) can be obtained by taking the derivative

$$\theta = \frac{z}{N} \frac{\partial \ln \Xi}{\partial z} \tag{60}$$

Inserting Eq. (59) into Eq. (58) one obtains

$$\theta = \frac{(1 - u + \lambda u)z}{2z(1 - u + \lambda u) + \lambda(1 - zu)} \tag{61}$$

In the case of no interactions $\Delta E = 0$, one has $u = 1$, and the isotherm simplifies to the known Langmuir isotherm

$$\theta = \frac{Ka}{1 + Ka} \tag{62}$$

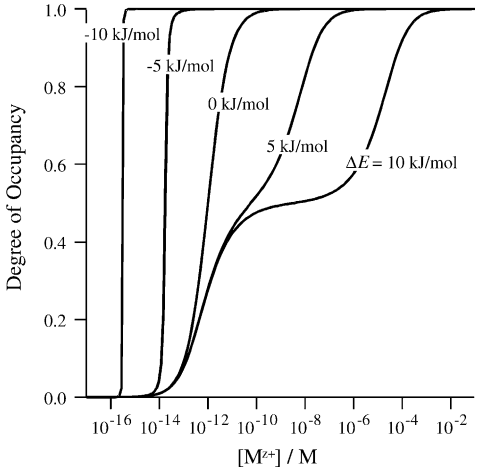

Fig. 21. Metal ion binding isotherms of an infinitely long linear receptor for different pair interaction energies. The microscopic binding constant is taken as $K = 10^{12}\ M^{-1}$.

For repulsive (anti-cooperative) interactions $\Delta E > 0$, this isotherm develops a characteristic plateau at $\theta = 1/2$. Examples are shown in Fig. 21. At low metal ion activity, the degree of occupancy is low, and the sites bind the metal ions independently. When one approaches half-occupancy, the system minimizes its free energy by occupying every second binding site.

The result is a highly ordered state of alternating occupied and empty sites (Fig. 22a). When the ion activity is increased further, the empty sites are filled as well. However, full occupancy is reached at much higher metal ion activities, as the energy of two nearest neighbour interactions have to be overcome. The alternating ordered structure arises due to the interactions in the receptor, and a completely disordered state is obtained in the absence of interactions (Fig. 22b).

In the case of attractive (cooperative) interactions $\Delta E < 0$, the isotherm rises in a very narrow region. Since metal ions attract, they form clusters along the chain separated by empty regions (Figs. 21 and 22c). While this situation does resemble a first-order phase transition, a genuine thermodynamic phase transition is not found within this model. To clarify the relation between the isotherms for the infinite chain receptor and a receptor with few sites discussed above, let us discuss the isotherms for the bimetallic helicate $[Ln_2(\mathbf{L24})_3]^{6+}$. These isotherms are shown for different interaction energies in Fig. 23. Obviously, the overall behavior is quite similar to that found for the linear chain. However, this case is normally described in terms of the equilibrium constants, which are also reported in Fig. 23 (right).

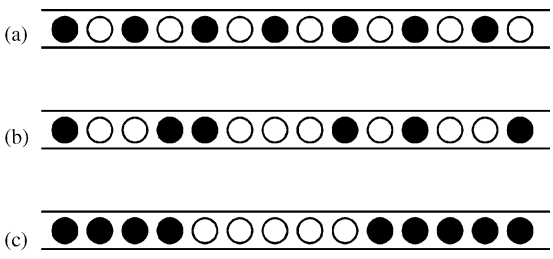

Fig. 22. Characteristic structures of the linear receptor at intermediate occupancy: (a) alternating arrangement for repulsive (anti-cooperative) interactions ($\Delta E > 0$), (b) random arrangement without interactions ($\Delta E = 0$), and (c) clustering of equally occupied sites for attractive (cooperative) interactions ($\Delta E < 0$).

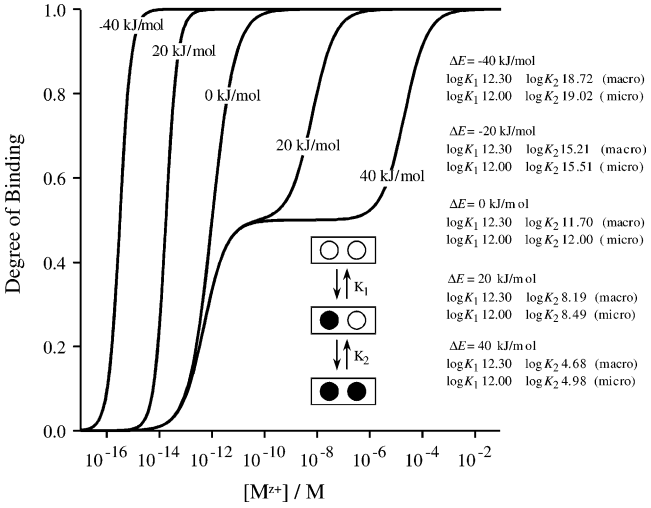

Fig. 23. Metal ion binding isotherms of a bimetallic linear receptor for different pair interaction energies. The microscopic binding constant $K_1 = 10^{12}\ M^{-1}$.

In the case of vanishing interactions (no cooperativity, $\Delta E = 0$), the isotherm is again of the Langmuir type. In this case the microscopic equilibrium constants for both sites are the same, while the macroscopic constants are separated by the statistical factor. For repulsive interactions (negative cooperativity, $\Delta E > 0$) an intermediate plateau develops at half occupancy. The equilibrium constants split now substantially, because once a site is occupied by a metal ion, the binding to the second site becomes less favorable. For attractive interactions (positive cooperativity, $\Delta E < 0$) the isotherm becomes steeper. The equilibrium constants are now reversed, as binding of the first metal ion facilitates the binding of the second.

The main difference between the two-site receptor and the infinite chain is that the effect of interactions is weaker in the bimetallic helicate than in the infinite chain, and larger interaction energies are needed to reach a comparable splitting in the bimetallic helicate. Moreover, mathematical forms of the isotherms are different. In the bimetallic (or multimetallic) helicate the isotherms can be represented in terms of the classical chemical equilibrium relations, while a more complicated expression is necessary for the infinite chain (Eq. (61)).

The same model can be applied to a mixture of two metal ions, provided the concentration of both metal ions is sufficiently high. Under these conditions, all sites of the receptor are occupied, but the relative proportion of the metal ions may change. The activity has to be now interpreted as the ratio of the concentrations of the two metal ions, and the interaction energy as the difference in the interaction energies between

the two different metals, namely

$$\Delta E = \Delta E_{11} + \Delta E_{22} - 2\Delta E_{12} \quad (63)$$

Thereby, ΔE_{ij} is the interaction energy between metal ions of type i and j. The fractional degree of occupancy must be now reinterpreted as the relative occupancy with the metal ion of type 2. The model results are instructive, and illustrated in Fig. 22. When the mutual interactions are all equal, one has $\Delta E = 0$, and the metal ion exchange happens along a Langmuir like isotherm. In particular, at half occupancy the different metal ions remain disordered along the receptor (Fig. 22b). When the repulsion between the different metal ions is weaker than among the ions of the same kind, one has $\Delta E > 0$, and the exchange isotherm forms an extended plateau where the receptor is occupied with both metal ions in an alternating fashion (Fig. 22a). On the other hand, when the repulsion between the different metal ions is larger than among the ions of the same kind, $\Delta E < 0$, a sudden transition between the fully occupied states of the receptor with either metal ion is expected (Fig. 22c).

The present *site-binding* model can be generalized to the situation, where empty sites on the receptor may coexist with sites occupied with different types of metal ions. The details of the analysis will be presented in a forthcoming publication. An example of such a situation for two very similar metal ions is shown in Fig. 24. The metal binding isotherm of the first metal ion M_1^{z+}, now also depends on the concentration of the second metal ion M_2^{z+}. At low concentration of M_2^{z+}, the binding of M_1^{z+} follows the classical binding isotherm with repulsive interactions, as shown in Fig. 21. When the concentration of M_2^{z+} is increased, the shape of the isotherm changes into a Langmuir-type isotherm. This situation is in accord with the observation that the exchange of two metal ions on a saturated receptor will follow the simple site-binding model, but with the interaction energy given by

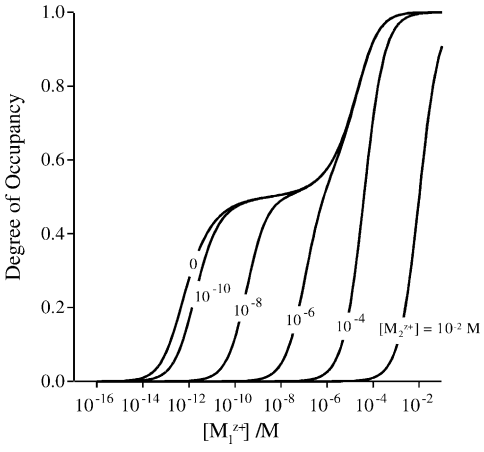

Fig. 24. Binding isotherms for competitive binding of metal ions 1 and 2 to a linear receptor. Both metals have the same binding constant $K_1 = K_2 = 10^{12}\ M^{-1}$ and same interaction energies $\Delta E_{11} = \Delta E_{12} = \Delta E_{22} = 20\ kJ\ mol^{-1}$. Due to symmetry, the binding isotherm for the second metal has the same appearance.

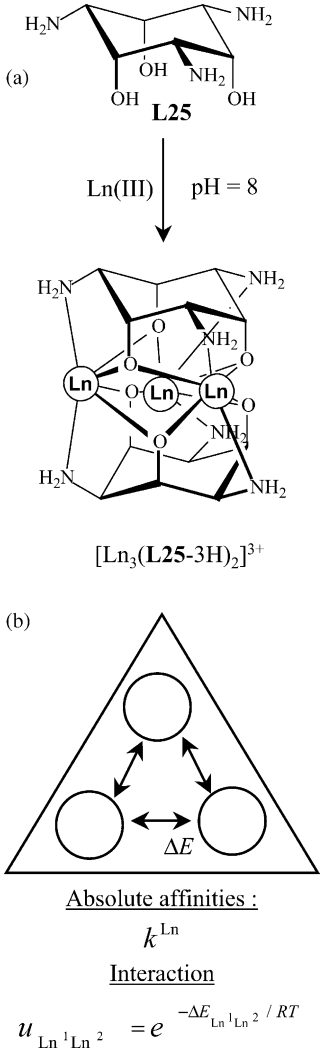

Fig. 25. (a) Formation and solution structure of $[Ln_3(\mathbf{L25}\text{-}3H)_2]^{3+}$ (each coordination sphere is completed by two water molecules which have been omitted for clarity) [52,53] and (b) associated thermodynamic *site-binding* model.

Eq. (63). Since the interactions in this model are symmetric, $\Delta E = 0$ is expected.

When the affinities and interactions between both metal ions are non-symmetrical, the behavior is quite a bit more complicated. Nevertheless, by controlling these interactions it might become possible to design specific arrangements of metal ions along linear receptors.

6.2. Two-dimensional sandwich complexes

The *cis*-inositol **L25** reacts with three Ln(III) to give the two-dimensional D_{3h}-symmetrical trimetallic sandwich complex $[Ln_3(\mathbf{L25}\text{-}3H)_2]^{3+}$ (Fig. 25) [52,53]. The pH-dependent constants $\beta_{x(3-x)2-6}$ associated with equilibrium (64) for the formation of the complexes $[(Ln^1)_x(Ln^2)_{3-x}(\mathbf{L25}\text{-}3H)_2]^{3+}$ (x = 0, 1, 2, 3) can be transformed into conditional stability constants $\beta_{x(3-x)2}$ at pH

= 8.0 (Eq. (65), $\alpha_{\mathbf{L25}}$ is the protonation coefficient of ligand **L25**), where the deprotonated trimetallic complexes are quantitatively formed in solution (Table 1) [52].

$$x[Ln^1]^{3+} + (3-x)[Ln^2]^{3+} + 2\mathbf{L25} \rightleftharpoons [(Ln^1)_x(Ln^2)_{3-x}(\mathbf{L25}-3H)_2]^{3+} + 6H^+, \quad \beta_{x(3-x)2-6} \tag{64}$$

$$\beta_{x(3-x)2} = \frac{\beta_{x(3-x)2-6}}{|H^+|^6 \alpha_{L25}} \tag{65}$$

If we reasonably assume that the free energy cost for the preorganization of two ligands **L25** is identical for the formation of any sandwich complexes $[(Ln^1)_x(Ln^2)_{3-x}(\mathbf{L25}\text{-}3H)_2]^{3+}$, it can be set to zero and the *site-binding* model shown in Fig. 25 holds. Eq. (66) gives the total free energy of complexation.

$$\Delta G_{tot}[Ln^1_x Ln^2_{3-x}] = -xRT\ \ln(k^{Ln^1}) - (3-x)RT\ \ln(k^{Ln^2}) + \tfrac{1}{2}x(x-1)\,\Delta E_{Ln^1Ln^1} + \tfrac{1}{2}(x-2)(x-3)\,\Delta E_{Ln^2Ln^2} + x(3-x)\,\Delta E_{Ln^1Ln^2} - RT\ \ln(s) = -RT\ \ln(\beta_{x(3-x)2}) \tag{66}$$

The usual straightforward mathematical transformation leads to Eq. (67) assuming that the interaction parameter is expressed as the Boltzmann factor $u_{Ln^iLn^j} = e^{-(\Delta E_{Ln^iLn^j}/RT)}$.

$$\beta_{3(3-x)2} = s(k^{Ln^1})^x (k^{Ln^2})^{3-x} (u_{Ln^1Ln^1})^{1/2x(x-1)} \times (u_{Ln^2Ln^2})^{1/2(x-2)(x-3)} (u_{Ln^1Ln^2})^{x(3-x)} \tag{67}$$

However, the number of parameters required for modelling a Ln^1/Ln^2 pair (k^{Ln^1}, k^{Ln^2}, $u_{Ln^1Ln^1}$, $u_{Ln^2Ln^2}$ and $u_{Ln^1Ln^2}$, Eq. (67)) exceeds the amount of accessible experimental formation constants (β_{302}, β_{212}, β_{122} and β_{032}, Table 1). Therefore, a mathematical solution requires that

Table 1
Formation constants of homo- and heterotrimetallic complexes $[(Ln^1)_x(Ln^2)_{3-x}(\mathbf{L25}\text{-}3H)_2]^{3+}$ (Ln^1, Ln^2 = Nd, Sm, Eu) [52]

Complex	$\log(\beta_{x(3-x)2-6})$[a]	$\log(\beta_{x(3-x)2})$[b]	$\log(\beta_{x(3-x)2})$[c]
$[Nd_3(\mathbf{L25}\text{-}3H)_2]^{3+}$	−24.09(1)	21.91	21.91
$[Sm_3(\mathbf{L25}\text{-}3H)_2]^{3+}$	−19.29(1)	26.71	26.73
$[Eu_3(\mathbf{L25}\text{-}3H)_2]^{3+}$	−17.93(1)	28.07	28.10
$[Nd_2Sm(\mathbf{L25}\text{-}3H)_2]^{3+}$	−22.4(3)	23.6	23.97
$[NdSm_2(\mathbf{L25}\text{-}3H)_2]^{3+}$	−20.5(1)	25.5	25.57
$[Nd_2Eu(\mathbf{L25}\text{-}3H)_2]^{3+}$	−21.7(2)	24.3	24.43
$[NdEu_2(\mathbf{L25}\text{-}3H)_2]^{3+}$	−20.1(5)	25.9	26.49
$[Sm_2Eu(\mathbf{L25}\text{-}3H)_2]^{3+}$	−18.8(3)	27.2	27.69
$[SmEu_2(\mathbf{L25}\text{-}3H)_2]^{3+}$	−17.68(6)	28.32	28.15
$[NdSmEu(\mathbf{L25}\text{-}3H)_2]^{3+}$	−20.1(5)	25.9	26.35

[a] Experimental data obtained in water by potentiometry [52].
[b] Conditional formation constants at pH 8, calculated with Eq. (65).
[c] Formation constants computed with Eqs. (70)–(73) and absolute affinities taken from Table 2.

Table 2
Fitted values of $\log(k^{Ln})$ for the sandwich complexes $[Ln_3(\mathbf{L25}\text{-}3H)_2]^{3+}$ (Eqs. (70)–(73))

Complex	$\log(k^{Ln})$[a]	$\log(k^{Ln})$[b]
$[Nd_3(\mathbf{L25}\text{-}3H)_2]^{3+}$	7.30(2)	10.58(2)
$[Sm_3(\mathbf{L25}\text{-}3H)_2]^{3+}$	8.91(2)	12.19(2)
$[Eu_3(\mathbf{L25}\text{-}3H)_2]^{3+}$	9.37(3)	12.65(3)

[a] Computed with $\Delta E = 0\ kJ\ mol^{-1}$.
[b] Computed with $\Delta E = 18.7\ kJ\ mol^{-1}$.

$u = u_{Ln^1Ln^1} = u_{Ln^2Ln^2} = u_{Ln^1Ln^2}$, an assumption which is justified by the experimental exchange constants associated with equilibrium (68) (K_{exch}(NdSm) = 3(10), K_{exch} (NdEu) = 2(12) and K_{exch} (SmEu) = 5(10)) which roughly match the statistical value $K_{exch}(Ln^1Ln^2) = 9$ when $u = u_{Ln^1Ln^1} = u_{Ln^2Ln^2} = u_{Ln^1Ln^2}$ (Eq. (69)).

$$[(Ln^1)_3(\mathbf{L25}\text{-}3H)_2]^{3+} + [(Ln^2)_3(\mathbf{L25}\text{-}3H)_2]^{3+} \rightleftharpoons [(Ln^1)_2(Ln^2)(\mathbf{L25}\text{-}3H)_2]^{3+} + [(Ln^1)(Ln^2)_2(\mathbf{L25}\text{-}3H)_2]^{3+}, \quad K_{exch} \tag{68}$$

$$K_{exch}(Ln^1Ln^2) = 9\frac{(u_{Ln^1Ln^2})^4}{(u_{Ln^1Ln^1})^2(u_{Ln^2Ln^2})^2} \tag{69}$$

For any Ln^1/Ln^2 pair, four macroscopic constants (Eqs. (70)–(73)) hold for fitting three parameters k^{Ln^1}, k^{Ln^2} and u. Moreover, each equation is modulated by u^3, which prevents its independent determination. Its value is thus arbitrarily fixed to $u = 1$ (i.e. $\Delta E = 0$), and the fitted $\log(k^{Ln})$ show a drastic increase along the lanthanide series (Table 2).

$$\beta_{302} = \left(k^{Ln^1}\right)^3 u^3 \tag{70}$$

$$\beta_{212} = 3\left(k^{Ln^1}\right)^2\left(k^{Ln^2}\right)u^3 \tag{71}$$

$$\beta_{122} = 3\left(k^{Ln^1}\right)\left(k^{Ln^2}\right)^2 u^3 \tag{72}$$

$$\beta_{032} = \left(k^{Ln^2}\right)^3 u^3 \tag{73}$$

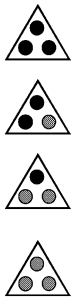

This behaviour is diagnostic for a strong, but classical electrostatic trend, in which the Ln–ligand interaction increases with decreasing size of the ionic radii [42]. According to ab initio calculations performed on closely related model complexes [54], the effective charge borne by a lanthanide ion in the complex $[(Ln^1)_x(Ln^2)_{3-x}(\mathbf{L25}\text{-}3H)_2]^{3+}$ can be estimated around +2, and this translates into $\Delta E \approx 18\ kJ\ mol^{-1}$ for the formation of $[Ln_3(\mathbf{L25}\text{-}3H)_2]^{3+}$ in water ($\varepsilon_r = 80$) assuming pure electrostatic repulsion between the metal ions considered as doubly-charged points [52]. A second set of $\log(k^{Ln})$ can be thus computed (Table 2) for which the electrostatic trend is obviously maintained. Although the experimental errors affecting K_{exch} (equilibrium (69)) is too large, and the sizes of Ln = Nd, Sm, Eu too

similar for definitely ruling out possible minor variations of $\Delta E_{Ln} i_{Ln} j$ in $[(Ln^1)_x(Ln^2)_{3-x}(\mathbf{L25}\text{-}3H)_2]^{3+}$, its approximate invariance and the chemical equivalence of the coordination sites dramatically limit the formation of pure heterotrimetallic bi-dimensional complexes [52].

7. Conclusions and perspectives

As demonstrated by *Ercolani* for hydrogen-bonded oligomers [55], self-assembled macrocycles [56] and metallosupramolecular edifices [29], classical thermodynamics is an efficient tool for rationalizing these new semantic concepts. This review parallely suggests that the terminology 'strict self-assembly of polymetallic helicates' can be indeed translated into more usual terms in coordination chemistry 'competitive thermodynamic formation of multimetallic one-dimensional oligomers'. This simplification is underlying in the concepts of 'maximum site occupancy' and 'maximum entropy' proposed for rationalizing metallosupramolecular self-assembly processes [7], but the belief in positively cooperative processes involving the assembly of charged cations has hindered the parallel development of rational and simple thermodynamic and/or kinetic models. Moreover, the current trend in chemical research toward applications has concomitantly restricted this field to the synthesis of novel and aesthetically appealing nanometric structures with potential functions, which are unfortunately rarely exploited. The basic modelling required for the programming of predetermined architectures and electronic properties is often considered as a luxury despite its crucial role for the specific introduction of different metal ions within organized polymetallic edifices. In this context, the self-assembly of helicates is symptomatic, since it took approximately 15 years to obtain adequate kinetic [37] and thermodynamic [29] arguments for rationalizing the original fascinating structural report of the double-stranded trimetallic helicates $[Cu_3(\mathbf{L1})_2]^{3+}$ [6]. If we limit our description to the thermodynamic behaviour, the combination of *Ercolani*'s model focusing on statistical repetitive binding [29], with the simple phenomenological *site-binding* model [43] provides an efficient tool for (i) the rational parametrization of helicate self-assembly, (ii) some predictions concerning the selective formation of heterometallic edifices and (iii) an unambiguous access to intermetallic interactions and cooperativity. The successful use of this method for the simultaneous modelling of the formation of the triple-stranded helicates $[(Ln^1)_x(Ln^2)_{2-x}(\mathbf{L24})_3]^{6+}$ and $[(Ln^1)_x(Ln^2)_{3-x}(\mathbf{L20})_3]^{9+}$ validates this approach [35], and extension toward larger objects (one-dimensional metallo-organic polymers, 2D and 3D metallosupramolecular architectures) is within reach. In this context, the recent use of the *Ising* model for the rough analyzes of the thermodynamic formation of a sophisiticated nonametallic $[Ag_9\mathbf{L}_9]^{9+}$ grid is encouraging, even though the detection of deviations from repetitive statistical binding remains qualitative [57]. The preliminary investigation of the parameters controlling the assembly of the much more simple sandwich complexes $[(Ln^1)_x(Ln^2)_{3-x}(\mathbf{L25}\text{-}3H)_2]^{3+}$ in this review provides the first quantitative data. Moreover, this simple model helps to highlight new challenges and perspectives. For instance, the absence of allosteric effects in the investigated lanthanide-containing helicates (i.e. $\Delta E_{intermetallic}$ is fixed for any lanthanide pairs), strongly limits the implementation of selective recognition processes, which are required for the preparation of pure heterometallic f–f′ complexes with novel optical and magnetic functions [42]. We therefore, do believe that metallosupramolecular chemistry could benefit from rational modelling using such simple thermodynamic models. It remains now to convince talented chemists around the world of the necessity of rationalizing the chemical pathways leading to their novel sophisticated and aesthetically appealing assemblies. The implementation of predetermined supramolecular functions, which have no counterpart in monometallic analogues, cannot be envisioned without these crucial efforts.

Acknowledgement

This work is supported through grants from the Swiss National Science Foundation.

References

[1] For reviews, see;
(a) D.S. Lawrence, T. Jiang, M. Levett, Chem. Rev. 95 (1995) 2229;
(b) C. Piguet, J. Incl. Phen. Macrocycl. Chem. 34 (1999) 361;
(c) D.L. Caulder, K.N. Raymond, J. Chem. Soc., Dalton Trans. (1999) 1185;
(d) S. Leininger, B. Olenyuk, P.J. Stang, Chem. Rev. 100 (2000) 853;
(e) G.F. Swiegers, T.J. Malefetse, Chem. Rev. 100 (2000) 3483;
(f) M. Fujita, K. Umemoto, M. Yoshizawa, N. Fujita, T. Kusukawa, K. Biradha, Chem. Commun. (2001) 509;
(g) P.D. Beer, E.J. Hayes, Coord. Chem. Rev. 240 (2003) 167.
[2] C. Piguet, G. Bernardinelli, G. Hopfgartner, Chem. Rev. 97 (1997) 2005.
[3] (a) A.F. Williams, C. Piguet, R. Carina, Transition Met. Supramol. Chem. 448 (1994) 409;
(b) A.F. Williams, R.F. Carina, L. Charbonnière, P.G. Desmartin, C. Piguet, Nato AST Ser. Phys. Supramol. Chem. (1996) 379.
[4] J.-M. Lehn, A.V. Eliseev, Science 291 (2001) 2331.
[5] (a) J.L. Atwood, L.R. MacGillivray, Angew. Chem. Int. Ed. 38 (1999) 1018;
(b) M. Boncheva, D.A. Bruzewicz, G.M. Whitesides, Pure Appl. Chem. 75 (2003) 621.
[6] J.-M. Lehn, A. Rigault, J. Siegel, J. Harrowfield, B. Chevrier, D. Moras, Proc. Natl. Acad. Sci. U.S.A. 84 (1987) 2565.
[7] J.-M. Lehn, Supramolecular Chemistry, VCH, Weinheim, New York, Basel, Cambridge, Tokyo, 1995.
[8] (a) C. Piguet, C. Edder, S. Rigault, G. Bernardinelli, J.-C.G. Bünzli, G. Hopfgartner, J. Chem. Soc., Dalton Trans. (2000) 3999;
(b) D. Imbert, M. Cantuel, J.-C.G. Bünzli, G. Bernardinelli, C. Piguet, J. Am. Chem. Soc. 125 (2003) 15698.
[9] C.M. Harris, E.D. McKenzie, J. Chem. Soc. (A) (1969) 746.
[10] For reviews, see;
(a) E.C. Constable, Tetrahedron 48 (1992) 10013;
(b) E.C. Constable, Prog. Inorg. Chem. 42 (1994) 67;

(c) E.C. Constable, in: J.L. Atwood, J.E.D. Davies, D.D. MacNicol, F. Vögtle (Eds.), Comprehensive Supramolecular Chemistry, Pergamon, Oxford, 1996 (Chapter 6) ;
(d) D.B. Amabilino, J.F. Stoddart, Chem. Rev. 95 (1995) 2725;
(e) D. Philp, J.F. Stoddart, Angew. Chem. Int. Ed. Engl. 35 (1996) 1154;
(f) M. Albrecht, Chem. Rev. 101 (2001) 3457.
[11] (a) J.-M. Lehn, A. Rigault, Angew. Chem. Int. Ed. Engl. 27 (1988) 1095;
(b) For a review on the terminology of self-assembly processes, see; J.S. Lindsey, New J. Chem. 15 (1991) 153.
[12] R. Krämer, J.-M. Lehn, A. Marquis-Rigault, Proc. Natl. Acad. Sci. U.S.A. 90 (1993) 5394.
[13] R.J. Motekaitis, A.E. Martell, R.A. Hancock, Coord. Chem. Rev. 133 (1994) 39.
[14] D.L. Caulder, K.N. Raymond, Angew. Chem. Int. Ed. Engl. 36 (1997) 1440.
[15] M. Shaul, Y. Cohen, J. Org. Chem. 64 (1999) 9358.
[16] C.R. Rice, C.J. Baylies, L.P. Harding, J.C. Jeffery, R.L. Paul, M.D. Ward, J. Chem. Soc., Dalton Trans. (2001) 3039.
[17] (a) E.C. Constable, A.J. Edwards, R. Raithby, J.V. Walker, Angew. Chem. Int. Ed. Engl. 32 (1993) 1465;
(b) C. Piguet, G. Hopfgartner, B. Bocquet, O. Schaad, A.F. Williams, J. Am. Chem. Soc. 116 (1994) 9092;
(c) V. Smith, J.-M. Lehn, Chem. Commun. (1996) 2733.
[18] (a) C. Piguet, J.-C.G. Bünzli, G. Bernardinelli, G. Hopfgartner, S. Petoud, O. Schaad, J. Am. Chem. Soc. 118 (1996) 6681;
(b) C. Piguet, E. Rivara-Minten, G. Bernardinelli, J.-C.G. Bünzli, G. Hopfgartner, J. Chem. Soc., Dalton Trans. (1997) 421;
(c) S. Rigault, C. Piguet, G. Bernardinelli, G. Hopfgartner, J. Chem. Soc., Dalton Trans. (2000) 4587;
(d) M. Cantuel, G. Bernardinelli, D. Imbert, J.-C.G. Bünzli, G. Hopfgartner, C. Piguet, J. Chem. Soc., Dalton Trans. (2002) 1929.
[19] N. André, T.B. Jensen, R. Scopelliti, D. Imbert, M. Elhabiri, G. Hopfgartner, C. Piguet, J.-C.G. Bünzli, Inorg. Chem. 43 (2004) 515.
[20] (a) D.A. McMorran, P.J. Steel, Angew. Chem. Int. Ed. Engl. 37 (1998) 3295;
(b) R. Clérac, F.A. Cotton, K.R. Dunbar, C.A. Murillo, I. Pascual, X. Wang, Inorg. Chem. 38 (1999) 2655.
[21] C. Provent, S. Hewage, G. Brand, G. Bernardinelli, L.J. Charbonnière, A.F. Williams, Angew. Chem. Int. Ed. Engl. 36 (1997) 1287.
[22] B. Hasenknopf, J.-M. Lehn, N. Boumediene, A. Dupont-Gervais, A. Van Dorsselaer, B. Kneisel, D.J. Fenske, J. Am. Chem. Soc. 119 (1997) 10956.
[23] D.P. Funeriu, J.-M. Lehn, K.M. Fromm, D. Fenske, Chem. Eur. J. 6 (2000) 2103.
[24] (a) A.F. Williams, C. Piguet, G. Bernardinelli, Angew. Chem. Int. Ed. Engl. 30 (1991) 1490;
(b) C. Piguet, G. Bernardinelli, B. Bocquet, A. Quattropanni, A.F. Williams, J. Am. Chem. Soc. 114 (1992) 7440.
[25] (a) A. Pfeil, J.-M. Lehn, J. Chem. Soc., Chem. Commun. (1992) 838;
(b) T.M. Garrett, U. Koert, J.-M. Lehn, J. Phys. Org. Chem. 5 (1992) 529.
[26] (a) K.E. Van Holde, Physical Biochemistry, second ed., Prentice-Hall, Englewood Cliffs, NJ, 1985;
(b) B. Perlmutter-Hayman, Acc. Chem. Res. 19 (1986) 90;
(c) A. Ben-Naim, J. Chem. Phys. 108 (1998) 6937.
[27] G. Scatchard, Ann. N.Y. Acad. Sci. 51 (1949) 660.
[28] A.V. Hill, J. Physiol. (London) 4 (1910) 40.
[29] (a) G. Ercolani, J. Am. Chem. Soc. 125 (2003) 16097;
(b) G. Ercolani, J. Phys. Chem. B 107 (2003) 5052.
[30] G. Koper, M. Borkovec, J. Phys. Chem. B 105 (2001) 6666.
[31] S. Blanc, P. Yakirevich, E. Leize, M. Meyer, J. Libman, A. Van Dorsselaer, A.-M. Albrecht-Gary, A. Shanzer, J. Am. Chem. Soc. 119 (1997) 4934.
[32] (a) See note 10 in [29a]; (b) T.H. Lowry, K.S. Richardson, Mechanism and Theory in Organic Chemistry, third ed., Harper & Row, New York, 1987, pp. 175–177; (c) δ is introduced here for the sake of simplicity. In [29], its value is included in σ_{sa}.
[33] R. Ziessel, A. Harriman, J. Suffert, M.-T. Youinou, A. De Cian, J. Fischer, Angew. Chem. Int. Ed. Engl. 36 (1997) 2509.
[34] S. Floquet, N. Ouali, B. Bocquet, G. Bernardinelli, D. Imbert, J.-C.G. Bünzli, G. Hopfgartner, C. Piguet, Chem. Eur. J. 9 (2003) 1860.
[35] K. Zeckert, J. Hamacek, S. Floquet, A. Pinto, M. Borkovec, C. Piguet, C. J. Am. Chem. Soc. 126 (2004) 11589.
[36] A. Marquis-Rigault, A. Dupont-Gervais, A. Van Dorsselaer, J.-M. Lehn, Chem. Eur. J. 2 (1996) 1395.
[37] N. Fatin-Rouge, S. Blanc, A. Pfeil, A. Rigault, A.-M. Albrecht-Gary, J.-M. Lehn, Helv. Chim. Acta 84 (2001) 1694.
[38] N. Fatin-Rouge, S. Blanc, E. Leize, A. van Dorsselaer, P. Baret, J.-L. Pierre, A.M. Albrecht-Gary, Inorg. Chem. 39 (2000) 5771.
[39] J. Hamacek, S. Blanc, M. Elhabiri, E. Leize, A. van Dorsselaer, C. Piguet, A.M. Albrecht-Gary, J. Am. Chem. Soc. 125 (2003) 1541.
[40] M. Elhabiri, J. Hamacek, J.-C.G. Bünzli, A.M. Albrecht-Gary, Eur. J. Inorg. Chem. (2004) 51.
[41] (a) M.T. Caudle, L.P. Cogswell, A.L. Crumbliss, Inorg. Chem. 33 (1994) 4759;
(b) M.T. Caudle, R.D. Stevens, A.L. Crumbliss, Inorg. Chem. 33 (1994) 6111;
(c) H. Boukhalfa, A.L. Crumbliss, Inorg. Chem. 39 (2000) 4318, and references therein ;
(d) I. Spasojevic, H. Boukhalfa, R.D. Stevens, A.L. Crumbliss, Inorg. Chem. 40 (2001) 49.
[42] J.-C.G. Bünzli, C. Piguet, Chem. Rev. 102 (2002) 1897.
[43] S. Floquet, M. Borkovec, G. Bernardinelli, A. Pinto, L.-A. Leuthold, G. Hopfgartner, D. Imbert, J.-C.G. Bünzli, C. Piguet, Chem. Eur. J. 10 (2004) 1091.
[44] N. Martin, J.-C.G. Bünzli, V. McKee, C. Piguet, G. Hopfgartner, Inorg. Chem. 37 (1998) 577.
[45] S. Petoud, J.-C.G. Bünzli, F. Renaud, C. Piguet, K.J. Schenk, G. Hopfgartner, Inorg. Chem. 36 (1997) 5750.
[46] R.F. Steiner, J. Chem. Phys. 22 (1954) 1458.
[47] R.A. Marcus, J. Phys. Chem. 58 (1954) 621.
[48] A. Katchalsky, J. Mazur, P. Spitnik, J. Polym. Sci. 23 (1957) 513.
[49] R.G. Smits, G.J.M. Koper, M. Mandel, J. Phys. Chem. 97 (1993) 5745.
[50] Y. Kawaguchi, M. Nagasawa, J. Phys. Chem. 73 (1969) 4382.
[51] J. de Groot, G.J.M. Koper, M. Borkovec, J. de Bleijser, Macromolecules 31 (1998) 4182.
[52] (a) R. Hedinger, M. Ghisletta, K. Hegetschweiler, E. Toth, A.E. Merbach, R. Sessoli, D. Gatteschi, V. Gramlich, Inorg. Chem. 37 (1998) 6698;
(b) D. Chapon, C. Husson, P. Delangle, C. Lebrun, P.J.A. Vottéro, J. Alloys Compd. 323–324 (2001) 128;
(c) D. Chapon, J.-P. Morel, P. Delangle, C. Gateau, J. Pécaut, Dalton Trans. (2003) 2745.
[53] N. Ouali, J.-P. Rivera, D. Chapon, P. Delangle, C. Piguet, Inorg. Chem. 43 (2004) 1517.
[54] G. Wipff, F. Berny, J. Chem. Soc., Perkin 2 (2001) 73.
[55] G. Ercolani, Chem. Commun. (2001) 1416.
[56] (a) X. Chi, A.J. Guerin, R.A. Haycock, C.A. Hunter, D.L. Sarson, J. Chem. Soc., Chem. Commun. (1995) 2563;
(b) G. Ercolani, J. Phys. Chem. B 102 (1998) 5699.
[57] A. Marquis, J.-P. Kintzinger, R. Graff, P.N.W. Baxter, J.-M. Lehn, Angew. Chem. Int. Ed. 41 (2002) 2760.